Defining the role of *Sabellaria alveolata* reefs as nursery areas for juvenile fish: first evidence from drone-based imagery and underwater visual census data

Daniele Ventura[1],*, Stanislas F. Dubois[2], Edoardo Cardella[1], Francesco Colloca[3], Francesco Tiralongo[4], Arnold Rakaj[5], Andre Bonifazi[5], Giovanna Jona Lasinio[6], Emanuele Mancini[7], Iacopo Bertocci[8], Edoardo Casoli[1], Gianluca Mancini[1], Tommaso Valente[1], Andrea Belluscio[1], Giandomenico Ardizzone[1], Maria Flavia Gravina[5]

[1]Department of Environmental Biology, University of Rome 'La Sapienza', V. le dell'Università 32, 00185 Rome, Italy

[2]IFREMER, DYNECO-LEBCO, Centre de Bretagne, Technopole Brest-Iroise, 1625 route de Sainte-Anne, CS 10070, Plouzane 29280, France

[3]Department of Integrative Marine Ecology, Stazione Zoologica Anton Dohrn, 00198 Rome, Italy

[4]Department of Biological, Geological and Environmental Sciences, University of Catania, 95129 Catania, Italy

[5]Department of Biology, University of Rome 'Tor Vergata', Via della Ricerca Scientifica s.n.c., 00133, Rome, Italy

[6]Department of Statistical Sciences, University of Rome 'La Sapienza', V. le dell'Università 32, 00185 Rome, Italy

[7]Department of Biological and Environmental Sciences and Technologies, DiSTeBA, University of Salento, 73100 Lecce, Italy

[8]University of Pisa, CoNISMa, Via Derna 1, 56126 Pisa, Italy

ABSTRACT: The biogenic reefs built by the honeycomb worm *Sabellaria alveolata* constitute priority habitats along Atlanto-Mediterranean coastal areas. Despite their wide extent and important ecological role, the nursery value of *S. alveolata* reefs remains unclear, and more information is needed to define how such structured habitats affect juvenile fish assemblages. In this study, habitat use by juveniles of 7 fish species was investigated by underwater visual census (UVC) at 3 study sites representing a gradient of complexity of *Sabellaria* reef habitats, spanning from a large and uniform reef to patchy and isolated small reef formations. *Sabellaria* reef metrics derived by drone-based cartography and GIS analysis were used to quantitatively monitor the seasonal structural changes occurring due to the natural dynamics of the reefs. We also tested the potential effect of *Sabellaria* habitats on the growth and relative condition factor (K_n) of white seabream *Diplodus sargus* juveniles. Five of the 7 surveyed species, especially sparid fishes, showed a clear preferential association with *Sabellaria* formations. Generalized additive modelling revealed a significant effect of the compactness ratio on estimated fish densities at high and low index values. The juvenile fish sampled on *Sabellaria* reefs exhibited higher values of K_n than those sampled on rocky habitats, supporting the hypothesis that structural complexity positively affected their condition. We provide evidence on habitat use by juveniles, suggesting that the presence of the *Sabellaria* reef may act as a nursery and affect local fish density in Mediterranean coastal waters.

KEY WORDS: Fish habitats · Habitat complexity · Biogenic reef · UAVs · Mediterranean Sea

1. INTRODUCTION

Marine coastal habitats provide several ecosystem services to nearshore human populations, including shoreline protection, commercial fisheries, recreational activities and nutrient cycling. The ecosystem goods and services provided by coastal habitats, such as seagrass beds, estuarine mudflats and saltmarshes,

are appreciably higher per unit area than those provided by terrestrial habitats (Costanza et al. 1997, Lefcheck et al. 2019). Coastal marine ecosystems encompass highly productive areas such as estuaries and bays that provide food resources and refuge for adult and juvenile fish and invertebrate species, contributing significantly to local and global biodiversity. As a result, they are widely recognized as nursery grounds for the growth and development of juvenile fish and shellfish (Paterson & Whitfield 2000, Beck et al. 2003). Over the last decades, a great effort has been made to define a standard framework to rigorously measure the importance of juvenile habitats as nurseries and to support their protection (Beck et al. 2003, Dahlgren et al. 2006, Nagelkerken et al. 2015). The nursery role hypothesis (NRH) formalized by Beck et al. (2001, p. 635) states: 'a habitat is a nursery for juveniles of a particular species if its contribution per unit area to the production of individuals that recruit to adult populations is greater, on average, than production from other habitats in which juveniles occur'. This definition constitutes a standard framework for rigorously measuring, comparing and categorizing nursery habitats through the ecological processes capable of supporting greater contributions to adult recruitment, depending on any combination of 4 factors: (1) density, (2) growth, (3) survival of juveniles and (4) movement to adult habitats. Therefore, the concept of a nursery must extend beyond simply the numbers of juveniles present but also may entail higher specific growth rates due to the abundance of food resources, higher survival owing to protection from predators and effective juvenile—adult linkage, resulting in more juveniles reaching the adult population (Heck et al. 2003). Although some aspects of the NRH have been contested (Sheaves et al. 2006, Baker & Sheaves 2007) and some modifications, therefore, suggested (Dahlgren et al. 2006, Nagelkerken et al. 2015), the core framework provided by the NRH for measuring juvenile habitat quality remains widely agreed upon.

However, despite wide acceptance of the NRH by marine biologists, fisheries managers and other stakeholders, and its recurrent use as justification for the protection and conservation of these specific widely distributed nursery habitats such as seagrass beds, estuaries, saltmarshes, mangrove forests, oyster beds and shallow rocky reefs (Nagelkerken et al. 2002, Dahlgren et al. 2006, Nagelkerken 2009, Litvin et al. 2018), little attention has been dedicated to other less common coastal habitats that can still play an important role in ecosystem functioning at the local scale. Among these, the role played by

temperate biogenic reefs made by polychaetes of the genus *Sabellaria* (Annelida, Sabellariidae) for juvenile fish remains unevidenced and poorly documented. The honeycomb worm *Sabellaria alveolata* (Linnaeus, 1767) is a common filter-feeding gregarious species that builds wave-resistant reefs of various types (i.e. mushrooms, pillows, barriers and platforms; Curd et al. 2019) by assembling mobile sand grains into solid tubes (Le Cam et al. 2011, Lisco et al. 2017). These worms use specific tentacular filaments calibrated to collect sediments and bioclast particles between 63 µm and 2 mm (belonging to the 'sand' class on the Wentworth scale; Wentworth 1922), resuspended by wave action, that are then cemented with proteinaceous adhesives to create a rigid but elastic tube (Le Cam et al. 2011, Deias et al. 2023). Due to their ability to transform soft-sedimentary habitats into engineered hard bioconstructions and to modulate resource availability to other species via structural modifications of the environment, *Sabellaria* worms are defined as 'ecosystem engineers' (Jones et al. 2018, 2021).

Sabellaria reefs are widespread along European Atlantic coasts, occurring on intertidal and subtidal shores of west Scotland to the south of Morocco (Dubois et al. 2002, Firth et al. 2015, Curd et al. 2019). In the Mediterranean Sea, important sabellariid reef formations can be found along the peninsular Italian coast (Gravina et al. 2018, Ingrosso et al. 2018, Bonifazi et al. 2019) and Sicily (Borghese et al. 2022, Sanfilippo et al. 2022), where they occur from the lower shore to the sublittoral fringe. *S. alveolata* can be regarded as the most important building organism along intertidal sandy coastal habitats, where it plays key ecological functions such as creating biodiversity hotspots (Dubois et al. 2006, Jones et al. 2020, Muller et al. 2021), increasing microphytobenthic primary production and promoting benthic—pelagic coupling (Jones et al. 2021) or filtrating phytoplankton biomass resulting in high clearance rates (Dubois et al. 2003). As a result, these reefs are listed under Annex I of the EC Habitats Directive (Habitat Directive 1992) as a marine habitat to be protected under the designation of 'Special Areas of Conservation'. Despite their relevant ecological role, sabellariid reefs are listed by the International Union for Conservation of Nature and Natural Resources (IUCN) as 'Data Deficient' in the European Red List of Habitats (Franzitta et al. 2022).

While the biodiversity of macrofaunal assemblages associated with *Sabellaria* reefs are well investigated (Bonifazi et al. 2019, Muller et al. 2021), very little is known regarding motile-associated megafauna using

this habitat, especially fish assemblages. In this context, defining the role of *S. alveolata* reefs in providing the specific ecosystem service of supporting juvenile life stages and thus sustaining adult fish populations is a fundamental requirement for characterizing and better managing coastal areas. It is well documented that habitat complexity provided by 3-dimensional structures constructed by marine polychaete worms in the families Sabellariidae (*S. alveolata, S. spinulosa*) and Terebellidae (*Lanice conchilega*) can serve as nursery grounds for larvae of several invertebrate species (Dias & Paula 2001, Dubois et al. 2006, Bremec et al. 2013, Seitz et al. 2014, Bonifazi et al. 2019, Aviz et al. 2021). However, regarding fish species, only a few studies reported *L. conchilega* (Rabaut et al. 2010) and *S. spinulosa* (Pearce et al. 2011a,b, Gibb et al. 2014) reefs as nursery grounds for certain fish species of commercial interest (e.g. flatfish) because of the high abundance of juveniles hosted. Since the role of *S. alveolata* reefs as nursery grounds remains unclear, the main objective of this study was to assess whether *S. alveolata* biogenic habitats play a key role in the Mediterranean fish population by investigating the density, growth and survival of juvenile fishes.

Over the past 70 yr, a variety of *in situ* non-destructive underwater visual census (UVC) techniques have been used to quantitatively estimate relative abundances, densities, sizes, biomass, habitat types and community structure of both adult and juvenile fish species in tropical (Brock 1954, Sale & Douglas 1981, Bohnsack & Bannerot 1986, St. John et al. 1990) and temperate areas (Harmelin-Vivien et al. 1985, 1995, Francour 1997, Vigliola & Harmelin-Vivien 2001, Cocheret De La Morinière et al. 2002, Ribeiro et al. 2005). Aside from the nature of the UVC method (e.g. point counts, strip transects, line transects, rapid visual counts) and the equipment used (e.g. SCUBA diving, baited remote underwater stereo-video stations, rotating video apparatus), UVC has proven helpful in expanding our knowledge of fish assemblages. However, no single approach is best suited for all circumstances, with each variant designed to examine a specific aspect of fish assemblages (Ribeiro et al. 2005). Moreover, the spatial distribution of juvenile fish assemblages is related to fine-scale variations in habitat structure (Harmelin-Vivien et al. 1995, Copp & Kovác 1996, Russo et al. 2007, Ventura et al. 2015), making the presence of adequate habitats critical during the settlement of juvenile stages. As a result of this site-specificity determined by the availability of microhabitats, juvenile fishes typically show regular and predictable patterns of dispersal from the

onset of settlement until recruitment to the adult population (García-Rubies & Macpherson 1995). Therefore, it is crucial to integrate habitat surveys in UVC sampling to better understand distribution patterns of organisms in relation to available habitats. Using a combination of observational techniques, spatial monitoring surveys can provide a more comprehensive perspective on fish ecosystems, aimed at describing specific aspects linked to species and habitat associations (Murphy & Jenkins 2010).

Underwater imagery derived from single photographs and video sequences acquired by underwater cameras mounted on remotely operated vehicles (ROVs) and autonomous underwater vehicles (AUVs), as well as acoustic data (side scan sonar, multibeam echo sounders), represent the most employed remote observational techniques used to support UVC (Kenny et al. 2003, Chabot et al. 2017, Egerton et al. 2018, Wetz et al. 2020, Cheal et al. 2021). Emerging technologies and recent advances in aerial imagery, such as multispectral satellite imagery (Collin et al. 2017) and airborne light detection and ranging (LiDAR) (Collin et al. 2018b), have the potential to increase our ability to accurately map remote or inaccessible areas, improving habitat discrimination within complex reef seascapes at large spatial scales. Also, at a finer scale and more specifically regarding *Sabellaria* reefs, low-cost but promising unmanned aerial vehicle (UAV) applications have been efficiently used to generate ultra-high spatial resolution orthophoto mosaics of honeycomb worm reefs, using a photogrammetric approach (Collin et al. 2018a, 2019, Ventura et al. 2018a, Jackson-Bué et al. 2021). Although these cartographic outputs can guide fish censuses more effectively in identified habitats of interest and finely depict reef topography to considerably reduce time and costs in underwater surveys, no attempts have been made to connect such mapping efforts to direct UVC data. Considering that data on the recruitment of demersal coastal fishes along the Italian coasts are still scarce and generally related only to the arrival of 0-group fishes in bays or lagoons (Vigliola et al. 1998), with no quantitative information available for specific microhabitat requirements such as those constituted by *Sabellaria* formations, we examined patterns of habitat utilization by juveniles of 7 fish species. Therefore, we investigated for the first time the role of *S. alveolata* reefs in providing an effective nursery habitat for juvenile fish among coastal waters by integrating GIS information derived from drone-based cartography with traditional UVC abundance estimates. We also explored the importance of *S. alveolata* reef structure on the recruitment

dynamics by associating the observed fish densities with reef shape complexity measured during winter (bioconstructions in the retrograding phase) and summer months (bioconstructions in the prograding phase). Finally, to provide a complete picture of the NRH, besides juvenile abundance patterns, we also investigated growth and body condition of white seabream *Diplodus sargus*. The interest in this species was driven by its socioeconomic importance, as it is exploited in local/artisanal and recreational fisheries throughout the year (Biagi et al. 2002, Tiralongo et al. 2021).

2. MATERIALS AND METHODS

2.1. Study site

This study was carried out along 1.3 km of sandy coastline in the Central Mediterranean Sea (Tyrrhenian Sea, west coast of Central Italy) south of Anzio Harbour, near the Natural Reserve of Tor Caldara. Along this coast, water turbidity is high during most of the year because of fine sandy sediments mixed with terrigenous particles derived from river runoff and high hydrodynamic force (high exposure to winds and wave energy from the southern sectors), making the area suitable for settlement by *Sabellaria alveolata*, which is well adapted to turbid systems and capable of maintaining its filtering activity even under high seston loads (Dubois et al. 2003).

Three sampling sites (labelled S1, S2 and S3, Fig. 1) were identified according to a gradient of structural complexity of *S. alveolata* bioconstructions. Large ball-shaped structures (up to 2 m diameter), some of them fused to form barriers and small platforms from the water surface up to 3 m depth, characterized the reef at Site S1 (41° 29′ 34.345″ N, 12° 35′ 9.088″ E). Due to its persistence and high ecological interest, this area has already been studied from geological (Moretti et al. 2019) and biological perspectives (Ventura et al. 2018a, Gravina et al. 2020). A smaller *S. alveolata* reef, mainly composed of mushroom-shaped formations (up to 1 m diameter) over a pebbly bottom from 0.5 to 3.5 m depth, characterized Site S2 (41° 29′ 18.224″ N, 12° 35′ 18.977″ E). Site S3 (41° 29′ 13″ N, 12° 35′ 19.172″ E) was characterized by reef type composed of isolated veneers and small pillow-shaped hummocks over a calcareous (upper Plicocene bioclastic calcarenites) substrate. Sites S1 and S2 mainly exhibited prograding formations (i.e. evidence of recent building activity and expanding biogenic formations). In contrast, Site S3 exhibited

retrograding phases (i.e. evidence of degraded reef portions and empty tubes), with biogenic formations showing signs of biofilm and epibiont cover, also represented in the surrounding bedrock covered by a dense carpet of photophilous algae. In this study, we cannot identify a standard control site with only rocky substrata since it is not present along the coast, especially considering reasonable distances from the other 2 sites (S1 and S2) where *Sabellaria* forms complex and stable reefs. In fact, the promontory at Site S3, which presents only small and isolated portions of *Sabellaria* growing on rocks, is the only stretch of coast with hard calcareous seabed. While areas displaying only rocky outcrops, such as Capo Circeo and Capolinaro, are present at around 60 km southward and 80 km northward, respectively, at such distances, other local factors related to oceanography and larval supply might have influenced juvenile densities, masking the effects of habitat type.

2.2. UAV-based imagery and GIS analysis

In late September 2019, an aerial survey with a low-cost UAV (Quanum Nova CX-20 equipped with a GoPro Hero 8 action camera) was used to produce a coarse map of the coast from an altitude of 120 m to identify the 3 study sites (Fig. S1 in the Supplement at www.int-res.com/articles/suppl/m735p103_supp.pdf). Subsequently, to effectively support the UVC survey, from October 2020 to November 2021, 6 high-resolution/low-altitude mapping missions were carried out both in fall–winter (September–February), following the main retrograding reef phase during autumnal storms, and in spring–summer (March–August), following the main prograding reef phase after larval recruitment focused during the spring (Ventura et al. 2021). Mapping missions were always carried out with calm sea conditions and low winds of <1 knot (0–1 on the Beaufort scale) to ensure optimal detection of targeted habitats and low local turbidity. Aerial mapping was conducted from an altitude of 30 m using a modified DJI Mavic 2 Pro UAV equipped with an additional L1/ L2 GNSS receiver with post-processing kinematics (PPK) capabilities to provide an improved cartography in terms of spatial resolution and positional accuracies of the 3 sites. This consumer-grade off-the-shelf UAV was a lightweight (0.9 kg) and easy-to-carry (322 × 242 × 84 mm, L × W × H) quadcopter equipped with a fully stabilized 3-axis gimbal Hasselblad L1D-20c camera RGB camera with a 1 inch (~2.54 cm) complementary metal
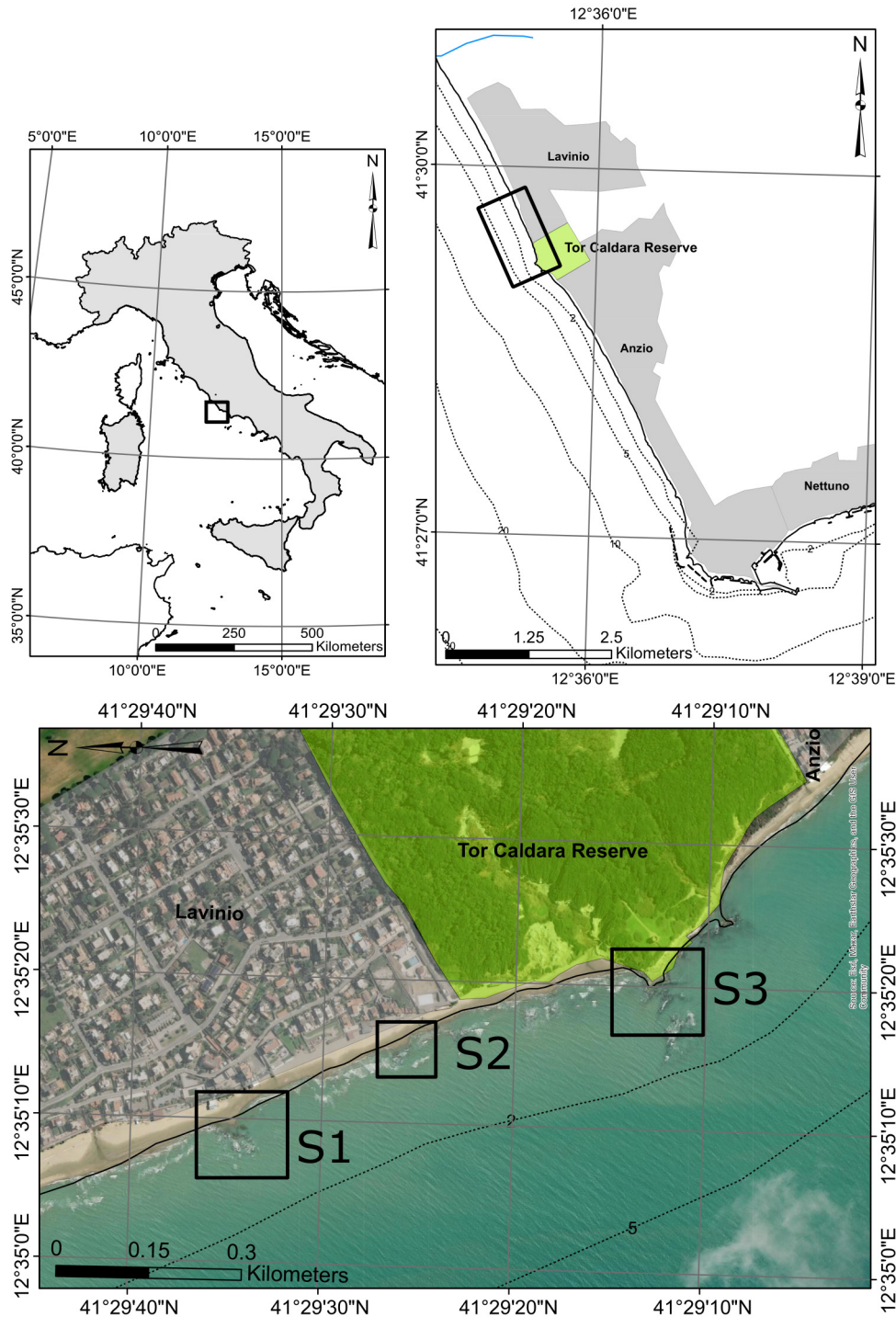
Fig. 1. Latium coast south of Rome (Central Tyrrhenian Sea), Italy, where the 3 study sites (S1, S2, S3) were located. The main urban complex and the limit of the Tor Caldara Natural Reserve are delineated by grey and green polygons, respectively. The dotted lines represent bathymetric depth contours

oxide semiconductor (CMOS) sensor. Each Li-Po Battery (3850 mAh) offered up to 30 min of flight time with good weather conditions and low wind. The Mavic 2 Pro Hasselblad L1D- 20c camera produced 20 megapixel format (5472 × 3648) photos, the sensor width was 13.2 mm, the actual focal length was 10.3 mm, and the UAV flew at a constant height of 30 m above mean sea level; we therefore applied the following formula to estimate the ground sample distance (GSD, the distance

between 2 consecutive pixel centres measured on the ground):

$$\text{GSD}_{\text{cm/pix}} =$$
$$\left(\frac{\text{Sensor width}_{\text{mm}} \times \text{Flight height}_{\text{m}}}{\text{Focal length}_{\text{mm}} \times \text{Image width}_{\text{pix}}}\right) \times 100 \quad (1)$$

to obtain a GSD of 0.7 cm per pixel, allowing an excellent identification of above- and below-water *S. alveolata* formations. The PPK routine was performed in Toposetter 2.0 Pro software, which allowed accurate georeferencing (less than 10 cm level accuracy in horizontal/vertical positioning) of the acquired imagery along the UAV track, using as input the UBX files recorded by the L1/L2 GNSS receiver mounted on the UAV and Rinex 3.03 files derived by a near Continuously Operating Reference Station (Ventura et al. 2023).

The UAV-based imagery was processed using Agisoft Metashape v 1.6.1, a low-cost Structure from Motion (SfM) photogrammetric software, to generate orthorectified photomosaics of the study area. SfM outputs included digital surface models of the mapped locations. Still, we did not include height information since the surface/elevation numerical model of the submerged part of the reef was affected by considerable inaccuracies due to water movements and light scattering. Orthophoto mosaics generated in Metashape were exported as raster images (GeoTIFF format, in the reference system WGS84/UTM zone 33 N, EPSG:32633) into a geographical information system using ArcMap 10.6 software (ESRI 2011) for subsequent classification by object-based image analysis (OBIA). Before classification, we reduced the pixel complexity by segmenting the orthophoto mosaics into more compact image objects through the mean-shift (MS) segmentation function available in the Spatial Analyst extension (Ventura et al. 2022, 2023). The spectral details, spatial details and minimum segment size parameters were set to 20, 18 and 800, respectively. After segmentation, we manually selected 30 image objects for each cover class (*Sabellaria* reef, sandy bottom and rocky substrata) as training samples to train the support vector machine (SVM) algorithm. The SVM model uses each band's mean and standard deviation to classify the image objects in the whole dataset. The classification results were verified using confusion matrices to compare OBIA results against 50 assessment points (20 ground-truthed and 30 random points visually sampled on the orthophoto mosaic). Validation points were first compared with the resulting classification, and the analyses included an overall map and per-class accuracies. We did not include the kappa coefficient because the

chance agreement is irrelevant in an accuracy assessment (Foody 2020). After cover class identification through OBIA, the Patch Shape extension available in the opensource plugin WhiteBox Tools v.1.4.0 (Lindsay 2014) was used to add indicators of shape complexity to the identified *S. alveolata* polygons, using 3 complementary metrics: (1) the compactness ratio (CR), which expresses the area:perimeter ratio, a measure of shape complexity, for a vector polygon where an increase in fragmentation leads to an increase in perimeter more rapidly than a change in area and therefore a decrease in CR; (2) the shape complexity index (SCI), which relates the shape of a polygon to that of an encompassing convex hull, defined as $\text{SCI} = 1 - A / Ah$ (where A is the area of the polygon and Ah is the area of the convex hull containing the polygon; as the shape of the polygon becomes more complex, the SCI approaches 1); and (3) the hole proportion (HP), which calculates the proportion of the total area of the holes in a polygon relative to the area of the hull of the polygon. It can be a valuable measure of shape complexity or patch discontinuity (Lindsay 2014). Mean values of CR, SCI and HP were derived using all the polygons attributed to *S. alveolata* reef for each study site and survey period. The percentage cover for each seabed class was calculated by dividing the area covered by the respective polygon by the total mapped area of the site. The aerial mapping mission was conducted using precise GPS information, ensuring that the total mapped area remained constant throughout summer to winter surveys.

2.3. UVC Sampling

Data on juvenile fish abundance and microhabitat use were collected twice per month from October 2020 to November 2021 by UVC. Censuses were carried out between 11:00 and 15:00 h and in a depth range of 0.3–2.5 m. To standardize the sampling effort, the UVC was carried out along predefined pathways, previously defined on UAV cartography, with different lengths according to the extent and complexity of each site, to cover an area of 600 m^2 (200 m L × 3 m W) at Sites S1 and S3 and an area of 570 m^2 (190 m L × 3 m W) at Site S2. One snorkeler swam slowly following the reef border while simultaneously recording all individuals within a fixed distance of 1.5 m per side. This distance was chosen because of the limited maximum horizontal underwater visibility and the small sizes of juveniles. To follow the correct path during each UVC survey, the snorkeler was equipped with a real-time track system through a water-resistant tablet running the GPS Log-

gerPro App, directly mounted on the marker buoy. The number of individuals of 7 target species (the white sea bream *Diplodus sargus*, the sharpsnout sea bream *D. puntazzo*, the two-banded sea bream *D. vulgaris*, the salema *Salpa sarpa*, the European sea bass *Dicentrarchus labrax*, the shi drum *Umbrina cirrosa* and the sand smelt *Atherina hepsetus*). time of the day, tide level and preferred habitat type according to 2 main categories (*S. alveolata* reef and hard substrata encompassing rocks with photophilic algae, pebbles and gravel) were recorded. When juveniles were observed for more than 5 min on a specific substrate type, we considered it a preferred substratum, as young juveniles typically show strong site-specificity; the microhabitat in which they were found was therefore assumed to be the one they preferentially used (García-Rubies & Macpherson 1995, Macpherson 1998).

Size classes for sparid fishes were chosen to define 3 principal periods of juvenile ontogenetic development (Macpherson 1998, Vigliola et al. 1998): settlement phase (smallest juveniles, 10−20 mm total length, TL), intermediate phase (medium-sized juveniles, 20−45 mm TL) and pre-dispersal phase outside the surveyed nursery areas (large juveniles, 45−66 mm TL). For other species, fish sizes were recorded in 30 mm size intervals. Plastic tablets with fish silhouettes and a ruler attached to the end of a meter stick were used to reduce magnification errors in estimating fish length (Bohnsack & Bannerot 1986, Harmelin-Vivien et al. 1995). When large shoals were observed, the count was carried out later in the lab, using FULL-HD (1920 × 1080 pixels) frames captured from video footage acquired by a Sony Alpha 6000 camera within a Sea Frog polycarbonate housing.

2.4. Estimation of condition factor and growth of *Diplodus sargus*

To determine the role of S. *alveolata* reef on condition of *D. sargus* juveniles, 173 fish (ranging from 16 to 66 mm TL) were collected from May to August 2021 at the 3 sites, using specific hand-nets with a 5 mm mesh size. We adapted the sampling effort proportionally to the extent of the total cover of the habitats (i.e. *S. alveolata* reef dominant at Sites S1 and S2; other hard substrates encompass rocks, pebbles and gravel, mainly represented at Site S3) to ensure comparable fish samples between sites. Therefore, we collected *D. sargus* juveniles on *S. alveolata* at Sites S1 and S2, whilst juveniles associated with rocky areas were sampled only from Site S3. Monthly size distributions of *D. sargus* juveniles were estimated for each sam-

pling site and preferential habitat to estimate growth variation over time. Considering the different extents of the 2 main habitat types at each site and the selective sampling method, the site could be used as a proxy for associating juveniles with the 2 main habitat types (*Sabellaria* and rocky substrata). Moreover, juveniles of *D. sargus* were never found free-swimming in sandy areas but were always sampled in small shoals, stationary in proximity to the 2 substrata considered. Analysis of covariance (ANCOVA) and linear regressions were used to test for slope differences between juvenile growth rate and habitat type.

The relative condition factor K_n was used to study the variation in juvenile condition while avoiding the effect of length (Ferraton et al. 2007). For each specimen, TL (in cm) and the eviscerated wet body weight (W_e, in g) were used to compute the formula as follows:

$$K_n = \frac{W_e}{W_{e'}} \qquad (2)$$

where W_e is the measured individual eviscerated weight and $W_{e'}$ is the estimated eviscerated weight from the $\log_{10}W_e - \log_{10}TL$ relationship ($W_{e'} = 10^{-\text{intercept}} \times TL^{\text{slope}}$).

2.5. Data analysis

Juvenile fish densities (*D*, expressed in the number of juveniles per 100 m^2) were estimated using UVC data as follows:

$$D = \frac{n_i}{W \times L} \qquad (3)$$

where n_i is the number of individuals detected, *W* is the path width (in metres), and *L* is the path length (in metres). Generalized additive models (GAMs) were used to investigate the influence of reef metrics on juvenile fish densities among the 3 study sites. GAMs are non-parametric extensions of generalized linear models (GLMs) that allow for non-linear relationships between predictor and response variables common to ecological data (Guisan & Zimmermann 2000, Zuur et al. 2007). The following equation gives a general GAM construction:

$$E[Y \mid X] = g^{-1}[X_a\beta + \Sigma s_k(X_k)] \qquad (4)$$

where E[Y|X] is the expected value of the response variable (log-transformed fish densities) given all independent information, *g* is a link function, X_a is a set of predictors linearly related to the dependent variable.

At the same time, X_k represents one of the K predictors not linearly related to the dependent variable, and S_k is a smooth function of the predictor variable X_k. A GAM with Gaussian distribution (with identity link function) was fit with a cubic regression spline as a smooth function using the 'mgcv' library in R version 4.2.1 (Wood 2001). Smooth functions were used to model the relationship between the response variable and the reef metrics estimated from UAV-based cartography. In the current study, cubic splines were restricted to a maximum of 5 knots for the full set of independent variables (i.e. site, species, size class, season, tide level, *Sabellaria* reef cover, substratum type, CR, SCI and HP) to prevent overfitting (Dance & Rooker 2016). Independent variables influencing juvenile densities were selected for the final model using a backwards stepwise procedure based on minimizing Akaike's information criterion (AIC), which measures goodness of fit while accounting for model complexity (number of variables). The approximate significance of the smoothed predictor (p-value) was used to guide the backward selection procedure, where the variable with the highest p-value (>0.05) was removed first. When removing a predictor returned a model with a smaller AIC (with ΔAIC > 2 between models), the same variable was excluded from the analysis. Stepwise selection continued until removing any remaining predictors increased the model AIC (Anderson et al. 1998). Non-significant (p > 0.05) terms retained in the final model were removed if model AIC was comparable (<2) after removal. In addition, as a secondary criterion to AIC, the overall model fit was assessed with percent deviance explained: DE = [(null deviance − residual deviance) / null deviance] × 100. The relative influence of each independent variable was assessed by removing each variable individually from the final model and comparing the percent change in DE (ΔDE) and change in AIC (ΔAIC). The 'gam.check' tool of the 'mgcv' package (Wood 2015), which plots the deviance residuals against approximate theoretical quartiles of the residual deviance distribution according to the fitted model, was used to check the model's residuals. Models with overdispersed and anomalous distributions of residuals were discarded. Significant differences for either fish habitat/site association and K_n were tested with a non-parametric Wilcoxon signed-rank test using the 'wilcox.test' function in the 'rstatix' package. The Bonferroni correction was applied to the resulting p-values to account for the influence of multiple tests. Results of the tests, expressed with significance codes, were plotted using the R packages 'ggpubr' (Kassambara 2020) and 'ggsignif' (Ahlmann-Eltze & Patil 2021).

3. RESULTS

3.1. *Sabellaria* reef metrics and their relationship with juvenile densities

The UAV-based orthophoto mosaics generated after SfM processing showed a spatial resolution of 0.66 cm pixel^{-1} (Fig. 2; Fig. S2). The high level of detail supported the UVC sampling by providing the snorkeler with accurate cartographic support that was helpful for survey management and data acquisition. The OBIA classification approach effectively identified the most important features of the coastal zones, including *Sabellaria* reefs, resulting in an overall mean (±SD) accuracy of 86.9 ± 0.3%. Major landcover misclassification errors involved spectral confusion among the class 'rocks with algae' with a total of 8.16 and 16.3% of samples interpreted as *S. alveolata* reef and sandy bottoms, respectively (overall producer and user accuracies are reported in Table S1). *S. alveolata* reef cover at Sites S1 (Wilcoxon signed-rank test; W = 3986, p = 0.0001) and S2 (W = 2257, p = 0.01) significantly differed from Site S3 considering both the winter and summer months. Site S1 exhibited the most considerable reef extent (2056 m^2) in summer, covering more than 33% of the whole area, whilst only limited *S. alveolata* reef bioconstructions were reported at Site S3, with an average cover of 5.2% throughout the year (Table 1). Generally, we observed a reduction in *S. alveolata* reef cover (up to 10% at Site S1) with an increase in the areas covered by sandy bottoms from summer to winter due to natural erosion of the bioconstructions and sand deposition during severe storms occurring more frequently from late summer.

The *S. alveolata* reef metrics CR, SCI and HP, derived after polygon delineation based on OBIA classification, exhibited large habitat variability among sites and seasons (Fig. 3). Generally, the 3 metrics showed significative differences from summer to winter months, denoting their ability in detecting natural dynamics of *S. alveolata* reefs. Site S1 showed the highest CR among the studied reefs both in summer and winter, being well-structured with a compact shape denoting reef stability. High CR values at Site S1 corresponded to a reef composed of large and continuous colonies (high surface for low perimeter) that can offer a more stable structure capable of withstanding the intensity of wave action and little prone to retrograding phase in winter. As expected, smaller CR values indicated smaller and more fragmented reef structures at Sites S2 and S3. Consequently, SCI increased significantly at Sites S1 (Wilcoxon signed-
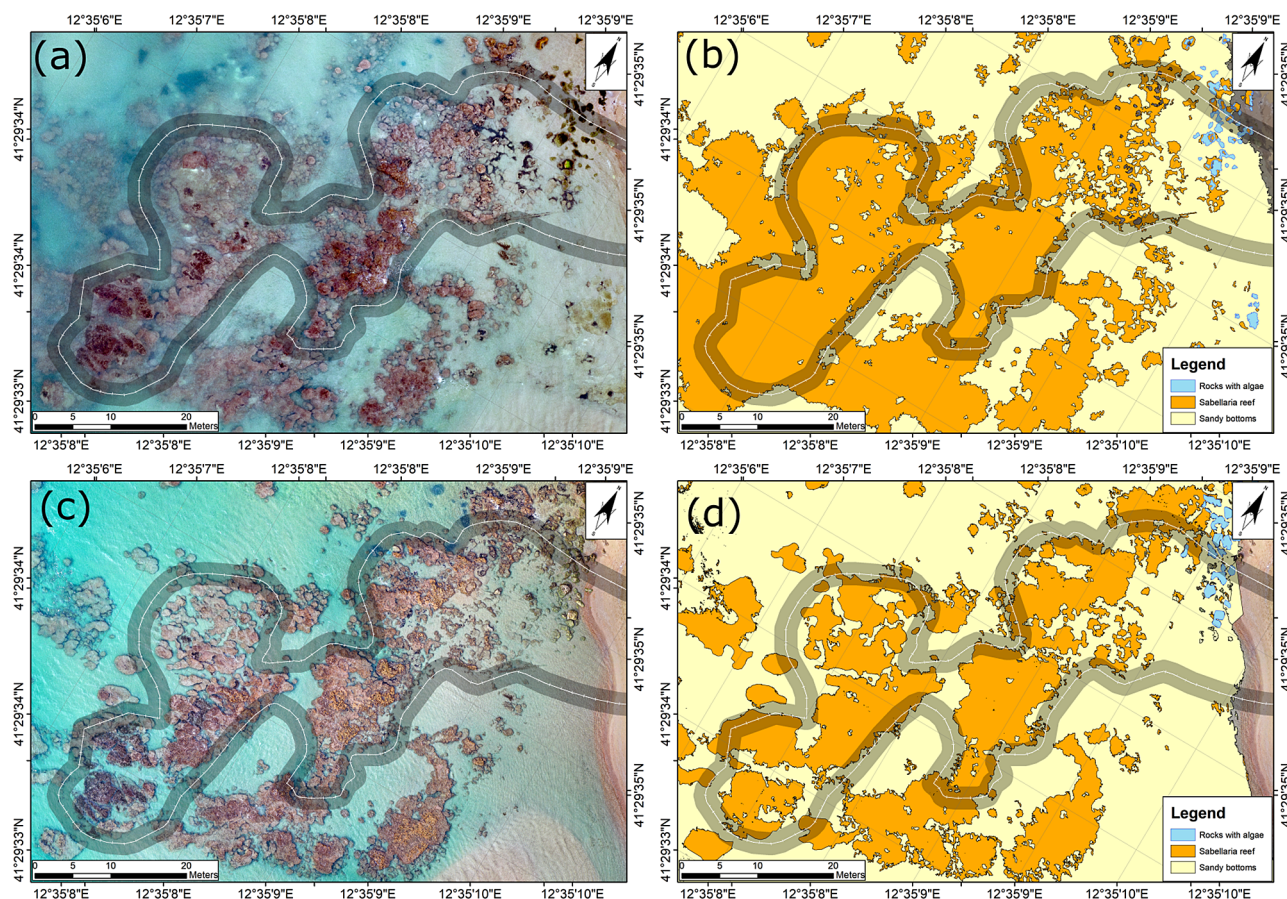
Fig. 2. High spatial resolution mapping of *Sabellaria* reef using unmanned aerial vehicle (UAV)-based orthophoto mosaic and imagery classification. (a) Orthophoto mosaic of Site S1 in summer with (b) the resulting classification derived by object-based image analysis (OBIA) leading to feature extraction and identification of the 3 main seabed cover classes (rocks with algae, *S. alveolata* reef and sandy bottom). (c) Orthophoto mosaic of Site S1 site in winter with (d) the resulting classification based on OBIA. Note the modification of reef boundaries and cover. The mean snorkeler's underwater visual census (UVC) path with a covered area of 600 m^2 (200 m length × 3 m width) derived by interpolation of multiple GPS tracks is reported in grey. The mapping and OBIA results of Sites S2 and S3 are reported in Fig. S1 in the Supplement

rank test; $W = 266$, p < 0.001) and S2 ($W = 589$, p < 0.001) from summer to winter, highlighting reef fragmentation. Conversely, Site S3 showed larger values of SCI in winter because of isolated reef formations constituted by small and low veneers between rocks, offering limited surfaces exposed to waves and therefore less prone to damage (Curtis 1975). At Sites S1 and S3, HP did not significantly increase in winter, whilst hole formation significantly ($W = 560$, p < 0.001) occurred in *S. alveolata* reefs at Site S2.

The final selected GAM (DE = 64.9%; pseudo-R^2 = 0.62) fitted on 256 observations included 4 retained variables, with species, site, size class, and CR being the most influential (Table 2). This model includes information on all relevant sources of variability when referring to juvenile density. The GAM formula we chose according to the AIC selection procedure and diagnostic plots are reported in Eq. (S1) and Fig. S3, respectively.

Table 1. Site overall extent (m^2) and reef habitat cover (%) at 3 sites (S1, S2, S3) as derived from unmanned aerial vehicle (UAV)-based aerial imagery object-based image analysis (OBIA) classification

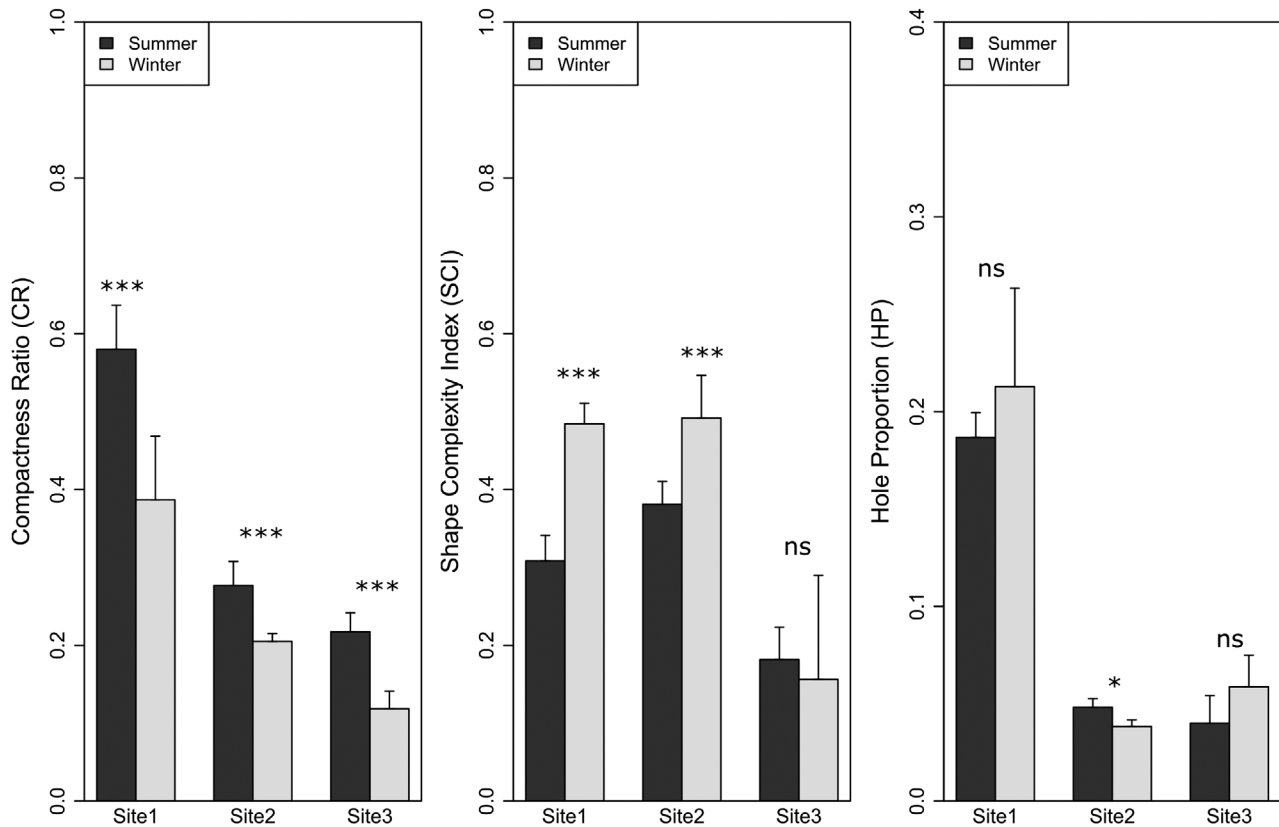| Site (m^2)	Season	Habitat m^2 (% cover)		
		Sabellaria reef	Sandy bottom	Rocks with algae
S1 (6100)	Summer	2056.4 (33.4)	4067.2 (66.1)	27.9 (0.5)
	Winter	1406.2 (23)	4709 (77)	0 (0)
S2 (2700)	Summer	354 (12.9)	2229.4 (81.4)	155.5 (5.7)
	Winter	267.6 (9.8)	2448.5 (89.5)	18.6 (0.7)
S3 (4100)	Summer	227.3 (7.2)	813.5 (25.9)	3103.1 (66.9)
	Winter	203.8 (3.3)	982.4 (29.7)	2954.5 (67)

Fig. 3. Mean values (±SE) of *Sabellaria alveolata* polygon-related reef metrics estimated after OBIA classification of UAV-based imagery. CR: compactness ratio; SCI: shape complexity index; HP: hole proportion. Wilcoxon signed-rank tests were used for pairwise comparisons. The alpha value was set at 0.05, and Bonferroni adjustment was applied for multiple comparisons. Significance codes: ***p < 0.001; *p < 0.05; ns = non-significant. See Fig. 1 (and Fig. S1 in the Supplement) for mapping results and visualization of *S. alveolata* reef polygons in different seasons

For all considered species, densities showed a significant negative effect from Site S1 to S3, which is especially marked for sparid species (higher for *Diplodus* spp. and minimum for *Salpa salpa*), *Dicentrarchus labrax* and *U. cirrosa*. Among *Diplodus* species, the white seabream *D. sargus* seemed the most influenced in terms of site selection, similar to *D. labrax*. The response plot of the non-linear term showed a sinusoidal trend indicating that juvenile fish densities were lowest at moderate values (0.3–0.5) of *Sabellaria* reef CR, whilst larger densities were reported both at lower (<0.3) and higher (>0.5) CR values (Fig. 4).

3.2. Temporal and spatial variability of juvenile fish

A total of 3395 juveniles belonging to the 7 target species were censused among the 3 sites over the whole study period. The most abundant species were 2 sparid fishes (*D. vulgaris* and *D. sargus*), accounting for 32.3 and 27% of the total juvenile assemblage,

respectively, followed by Atherinidae (*Atherina hepsetus*, 21.2%) and *Salpa salpa* (10.5%). *D. puntazzo*, *Umbrina cirrosa* and *Dicentrarchus labrax* were recorded occasionally, representing a small fraction of the assemblage (5.8, 2 and 1.3%, respectively). Within-month variation in juvenile density was high, especially for sparid fishes (Fig. S4). *D. sargus* and *D. vulgaris* were found mainly from late spring to mid-summer, whilst *S. salpa* and *D. puntazzo* were observed in winter. The other species (*A. hepsetus*, *D. labrax* and *U. cirrosa*) were censused mainly in late summer or early autumn.

During the summer months, juvenile density significantly differed from Sites S1 to S2 (Wilcoxon signed-rank test; $W = 3399$, p < 0.001) and from Sites S1 and S3 ($W = 3554$, p = 0.003), with the highest mean ± SD density of 14.3 ± 16.8 (n = 82) ind. 100 m^{-2} recorded at Site S1 (Fig. 5). The sea breams *D. sargus* ($W = 1645$, p < 0.001) and *D. puntazzo* ($W = 129$, p = 0.01) and the sea bass *D. labrax* ($W = 27$, p = 0.04) showed significant decreasing density values passing from

Table 2. Output of the generalized additive model on log-transformed juvenile densities (expressed in number of juveniles per 100 m^2), reporting the model's linear and non-linear terms. Note that the alpha value was set at 0.05, and the p-values of all the linear and non-linear terms are significant

— Linear terms —				
Explanatory variable	Estimate	SE	t	p
Intercept	4.4059	0.2326	18.944	<0.001
Site: S2	−0.507	0.2446	−2.073	0.039
Site: S3	−0.7244	0.2388	−3.033	0.003
Species: *Dicentrarchus labrax*	−2.6066	0.2904	−8.975	<0.001
Species: *Diplodus puntazzo*	−2.211	0.225	−9.828	<0.001
Species: *Diplodus sargus*	−2.4086	0.1857	−12.97	<0.001
Species: *Diplodus vulgaris*	−1.0024	0.2196	−4.565	<0.001
Species: *Salpa salpa*	−0.5664	0.2616	−2.165	0.031
Species: *Umbrina cirrosa*	−1.8902	0.3736	−5.059	<0.001
Size class: Medium	−0.3964	0.1143	−3.469	<0.001
Size class: Large	−0.6955	0.1516	−4.587	<0.001
— Non-linear (smooth) terms —				
Explanatory variable	edf	Ref. df	F	p
Complexity ratio (*Sabellaria* reef)	3.38	3.78	2.605	**0.0218**

Sites S1 to S3 (Fig. 6). Shi drum *U. cirrosa* juveniles were observed only at Site S1. The other sparid fishes (*D. vulgaris*, *S. salpa*) and the Mediterranean sand smelt *A. hepsetus* were censused with comparable mean densities at all sites.
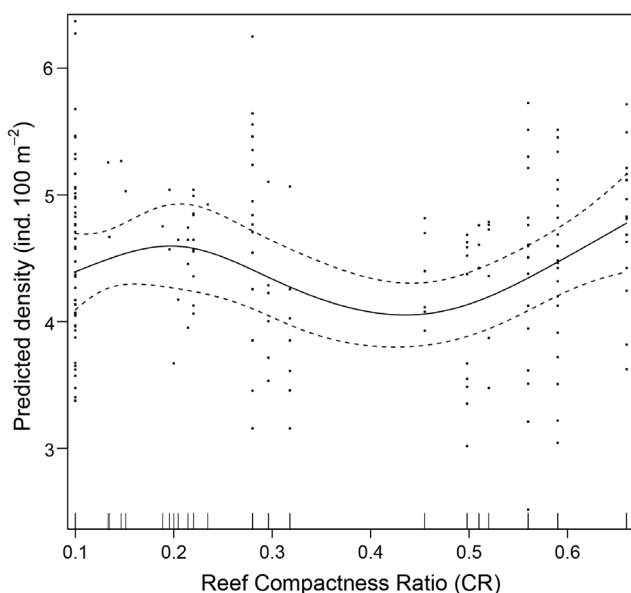

Fig. 4. Response plots showing the influence of the retained non-linear term (*Sabellaria alveolata* reef compactness ratio, CR) on juvenile fish densities among the 3 sites according to the final generalized additive model (GAM). Model fit was assessed with Akaike's information criterion (AIC) and % deviance explained (DE). Solid lines represent smoothed values; dotted lines represent 95% confidence intervals. N = 256 observations (site × species × size class)

3.3. Habitat use by juveniles

Juveniles of the genus *Diplodus* (*D. sargus*, *D. vulgaris*, *D. puntazzo*) showed a significant association with *S. alveolata* biogenic formations when compared to the other rocky habitats, mainly constituted by hard substrates covered by photophilic algae (Fig. 7). *U. cirrosa* juveniles were only reported in proximity to *S. alveolata* formations. Conversely, the mean densities of *A. hepsetus*, *D. labrax* and *S. salpa* juveniles did not differ among the 2 habitat types, with the latter mostly forming large shoals over rocky substrates. Small and medium-sized juveniles (2−5 cm TL) were observed prevalently (>70%) near *Sabellaria* formations (Fig. 8). This habitat association was particularly evident for sparid species (especially for *D. sargus*) and *D. labrax*, which represented almost all of the juveniles observed on *Sabellaria* reef, even several months after settlement. By contrast, large juveniles of *S. salpa* (7−8 cm TL) and *A. hepsetus* (2−3 cm TL) showed a preference for rocky substrates covered by photophilic algae.

3.4. Relative condition factor (K_n) and growth of *Diplodus sargus* juveniles

Monthly size distributions of the sampled *D. sargus* juveniles from May to August differed significantly between months and substrate type (Fig. 9a) in June (Wilcoxon signed-rank test; $W = 286$, p < 0.001) and July ($W = 55$, p = 0.004). *D. sargus* juveniles associated with *Sabellaria* reef at Sites S1 and S2 exhibited higher increases in monthly size (regression slopes were significantly different among habitat types in both slopes and intercepts (ANCOVA, regression slope: $F = 4.33$, df = 1, p = 0.03) than juveniles settling on other hard substrates at Site S3 (Fig. 9b).

K_n significantly differed (Wilcoxon signed-rank test; $W = 1396$, p < 0.001) in juvenile *D. sargus* living near *Sabellaria* reef compared to specimens collected on hard rocky substrates. These differences were particularly strong among small (25.3 ± 3.1 mm TL; $W = 70$, p < 0.001) and medium-sized (35.1 ± 4.8 mm TL; $W = 63$, p = 0.01) juveniles, whilst for larger juveniles (55.1 ± 4.7 mm TL), the effect of habitat on fish condition was not significant (Fig. 10).
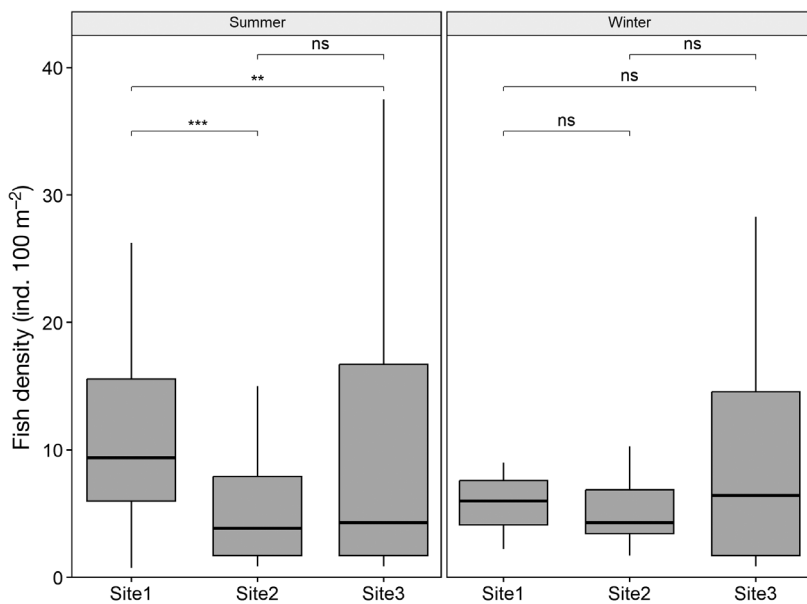
Fig. 5. Seasonal variation in juvenile fish densities (expressed as number of individuals per 100 m^2) recorded at the 3 sites from October 2020 to November 2021. Wilcoxon signed-rank tests were used for pairwise comparisons. The alpha value was set at 0.05, and Bonferroni adjustment was applied for multiple comparison. Boundaries of the boxes represent the 25th and 75th percentiles; solid line within the box is the median; error bars above and below the box indicate the 10th and 90th percentiles, respectively. Significance codes: ***p < 0.001; **p < 0.01; ns = non-significant

4. DISCUSSION

The function of shallow coastal habitats as essential nursery grounds for marine fishes has become an accepted ecological concept (Amara et al. 2007, Searcy et al. 2007). However, not all coastal areas are equally important as nursery grounds. Quality nursery habitats contribute disproportionately to the adult population by supporting increased densities, faster growth, better survival and successful movement of recruits to adult habitats (Beck et al. 2001). Juvenile fish densities, growth, survival and connectivity are essential indicators of juvenile habitat quality that must be understood in an ecosystem-based approach to implementing comprehensive fisheries management strategies (Beck et al. 2003, Schloesser & Fabrizio 2019). Therefore, the dynamics affecting essential fish habitats must be recorded accurately and extensively in marine monitoring surveys, especially in complex coastal environments where microscale variability may affect the estimates (Edgar et al. 2004). To date, this assessment is generally missing for temperate biogenic reefs made by the tube-building worm *Sabellaria alveolata*, which, analogously to other biogenic worm reefs, are considered hotspots of biodiversity capable of providing

refuge to an array of organisms, including hard- and sandy-bottom invertebrates (Bremec et al. 2013, Gravina et al. 2018, Ingrosso et al. 2018, Giangrande et al. 2020).

Our results indicated that juveniles of 5 commercially important species (*Diplodus sargus*, *D. puntazzo*, *D. vulgaris*, *Dicentrarchus labrax* and *Umbrina cirrosa*) preferentially use *S. alveolata* reef habitats with more cohesive reef structures that have little or no fragmentation, such as those occurring at Site S1. Fish densities were non-linearly linked to the CR metric, a common estimate of reef fragmentation: higher densities of juveniles were associated with high and low levels of reef CR, with lowest densities at moderate CR values. As expected, a massive, unfragmented and compact reef (i.e. high CR values) has the greatest effect on the density and diversity of juvenile fish. It offers shallow, sheltered areas with reduced hydrodynamic forces and lower predation rates (Ruiz et al. 1993). Paradoxically, a similar refuge effect can also be observed when reef habitat fragmentation is maximal (i.e. low CR values) due to an increase in faults and anfractuosities due to degradation of biogenic structures (Dubois et al. 2002, Stone et al. 2019). This effect has been demonstrated in macrofaunal diversity, where numerous small sessile epibionts colonized degraded and fragmented reef structures (Dubois et al. 2006, Bonifazi et al. 2019). Similarly, as shown in degraded coral reefs, prey vulnerability increases, leading to an initial rise in resource availability and productivity for a significant part of the reef fish community, particularly herbivores and invertivores (Brandl et al. 2016, Olán-González et al. 2023), confirming that habitat degradation allows the exploitation of novel resources by fishes that feed on macroinvertebrates such as juvenile sparid fishes (Ventura et al. 2017, 2018b).

Moreover, when the loss of one microhabitat type occurs due to reef degradation during winter storms, there is a simultaneous replacement by another microhabitat type, and, typically, massive *S. alveolata* structures are replaced mainly by sandy rubble on degraded reefs, and some juvenile fishes that prefer rubble microhabitats benefit from reef degradation. On the other hand, the lowest densities of juveniles
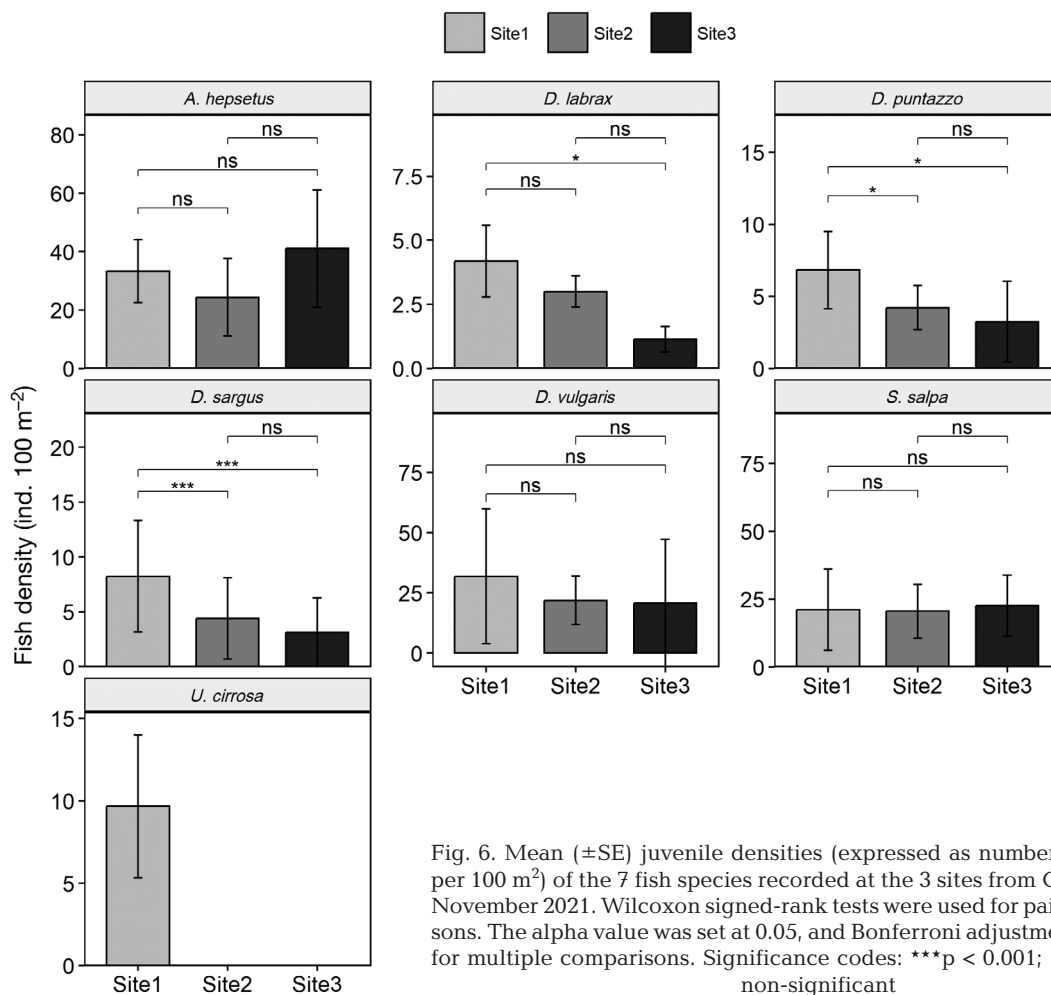
Fig. 6. Mean (±SE) juvenile densities (expressed as number of individuals per 100 m²) of the 7 fish species recorded at the 3 sites from October 2020 to November 2021. Wilcoxon signed-rank tests were used for pairwise comparisons. The alpha value was set at 0.05, and Bonferroni adjustment was applied for multiple comparisons. Significance codes: ***p < 0.001; *p < 0.05; ns = non-significant

reported at moderate CR values may be due to the transitional morphology of the reef between prograding and retrograding stages (Curd et al. 2019, Firth et al. 2021). This study shows that the refuge effects of *S. alveolata* habitats are just as important whether the reef is massive and little fragmented or made up of small, highly fragmented structures, providing valuable nursery grounds hosting high juvenile densities throughout the year. This result should have consequences in terms of management and restoration (Franzitta et al. 2022) of this reef habitat so as not to exclusively target extensive reefs (in size or surface area). Still, it should also make it possible to justify important ecological functions in nursery areas for the smallest and most fragmented biogenic reefs.

It should be noted that the predicted effect size is minimal (approximately 5 fish per 100 m²), especially considering the considerable measurement uncertainty characterizing UVC sampling. Moreover, the limited deviance explained by the CR term also suggested that the relationship was not particularly

strong. While accepting that structure does not significantly affect juvenile fish densities at the scales and extents examined here, our results confirmed that the reef, in all of its forms, acts as a preferential habitat for juveniles. Consequently, we can argue that *S. alveolata* reefs play an essential role as a nursery area for juvenile fish despite their degree of compactness and fragmentation. Similar results are reported for plant traits such as shoot density and aboveground biomass, which are only weakly correlated with the diversity of the associated fauna and may not provide good proxies for diversity for another engineered habitat constituted by eelgrass *Zostera marina* meadows (Muller et al. 2023). In fact, no significant differences were found between communities from the centres to the edges of the meadows, indicating that both habitats provide similar benefits to biodiversity and highlighting that the shape of the community was directly mediated by the presence of the meadow more than its health status (Muller et al. 2023).
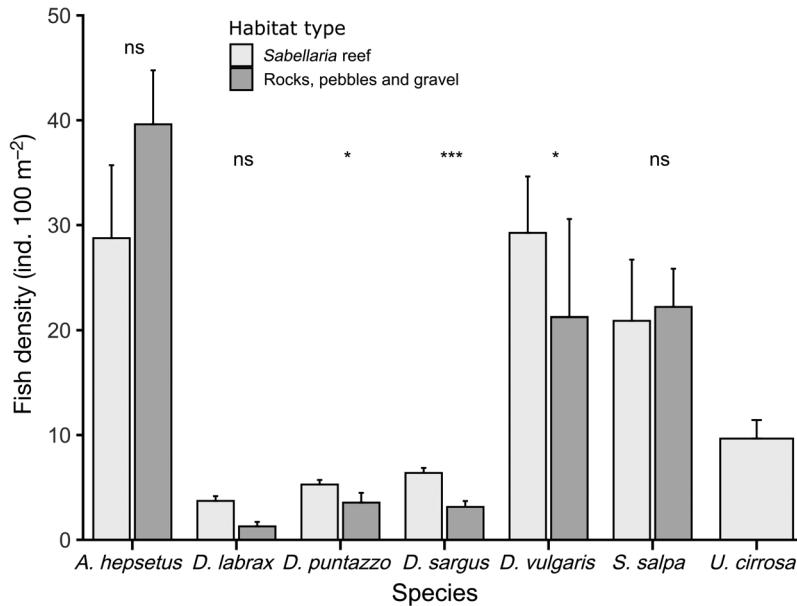
Fig. 7. Mean (±SE) juvenile densities (expressed as number of individuals per 100 m^2) of the 7 species recorded in relation to preferential habitat use. Wilcoxon signed-rank tests were used for pairwise comparisons. The alpha value was set at 0.05, and Bonferroni adjustment was applied for multiple comparisons. Significance codes: ***p < 0.001; *p < 0.05; ns = non-significant

Estimates of the ecological values of nursery areas, which are particularly important in monitoring the effects of fishing and protection strategies on the structure of coastal fish assemblages, are available for a variety of coastal benthic systems, including those supported by engineering species such as seagrasses (Jackson et al. 2001, Dorenbosch et al. 2004), mangroves (Mumby et al. 2004), oyster reefs (Beck et al. 2003) and other reef-building polychaetes such as *Lanice conchilega* (Rabaut et al. 2009, 2010), *Ficopomatus enigmaticus* (Méndez Casariego et al. 2004) and *S. spinulosa* (Reise 2012, Tillin et al. 2018). By contrast, virtually no data are available to quantify the importance of *S. alveolata* formations for coastal juvenile fish assemblages, especially in the Mediterranean Sea. Therefore, considering that the most common and widely accepted criterion for defining the nursery function of habitats is their ability to provide food and refuge (Paterson & Whitfield 2000), the efforts directed at evaluating habitat quality in the context of the nursery-role concept should not be limited to abundances, but should also take into account growth, survival and linkage (Beck et al. 2001, 2003, Dahlgren et al. 2006, Lefcheck et al. 2019). In this respect, we also evaluated the potential effects on growth rate and fish condition exerted by *S. alveolata* reefs compared to adjacent hard substrata. Fish condition is critical because it dramatically influences growth, reproduction and survival. Fish condition has

seldom been used to assess habitat quality in marine ecosystems, where most of the research dealt with differences in abundance and biomass between habitats (Lloret et al. 2002, Cantafaro et al. 2017). Although we quantified growth and K_n for a single sparid species (i.e. *D. sargus*), our results provided an important baseline for other species that utilized the *S. alveolata* reef as a nursery area. *S. alveolata* reef hosts a high diversity of associated fauna, including sessile (bivalves), burrower (tanaidaceans) and infaunal invertebrates (isopods, amphipods and polychaetes), which could themselves support other benthic infaunal assemblages and, in turn, provide food for fish, as confirmed by previous studies on feeding habits of sparid fishes (Sala & Ballesteros 1997, Costa & Cataudella 2007, Ventura et al. 2017, Bonifazi et al. 2018). The highest K_n and growth rate were reported for small and medium size classes of juveniles, as larger juveniles already expand their feeding ground outside the reef structures; the high density of small invertebrates offers a head start in development for juvenile fish exploiting reef habitats as feeding grounds. *S. alveolata* is also a potential food source that may directly influence the condition of fish: worms can be sucked out from their tubes by juveniles with enough suction power, such as sparids (Christensen 1978) or during reef destruction (i.e. during storms and periods of high wave energy). Considering, however, that juveniles of predators (*D. labrax*) were found at the same sites, the refuge effect from consumer pressure provided by shallow bottoms may be overestimated, suggesting that the refuge paradigm may be too simplistic for diverse and complex nursery grounds (Baker & Sheaves 2007). Thus, the factors that more likely influence the distribution of juvenile fishes in shallow water are probably related to the availability of food resources (Le Pape & Bonhommeau 2015).

In Mediterranean environments, especially inside complex communities such as seagrass meadows and biogenic reefs, UVC results can be affected by some typical sources of error linked to environmental conditions, such as water clarity that may affect the detectability of fishes (La Manna et al. 2021), the surveyed area dimensions (Jones et al. 2015), the census methodology (Pais & Cabral 2018), the trait of target
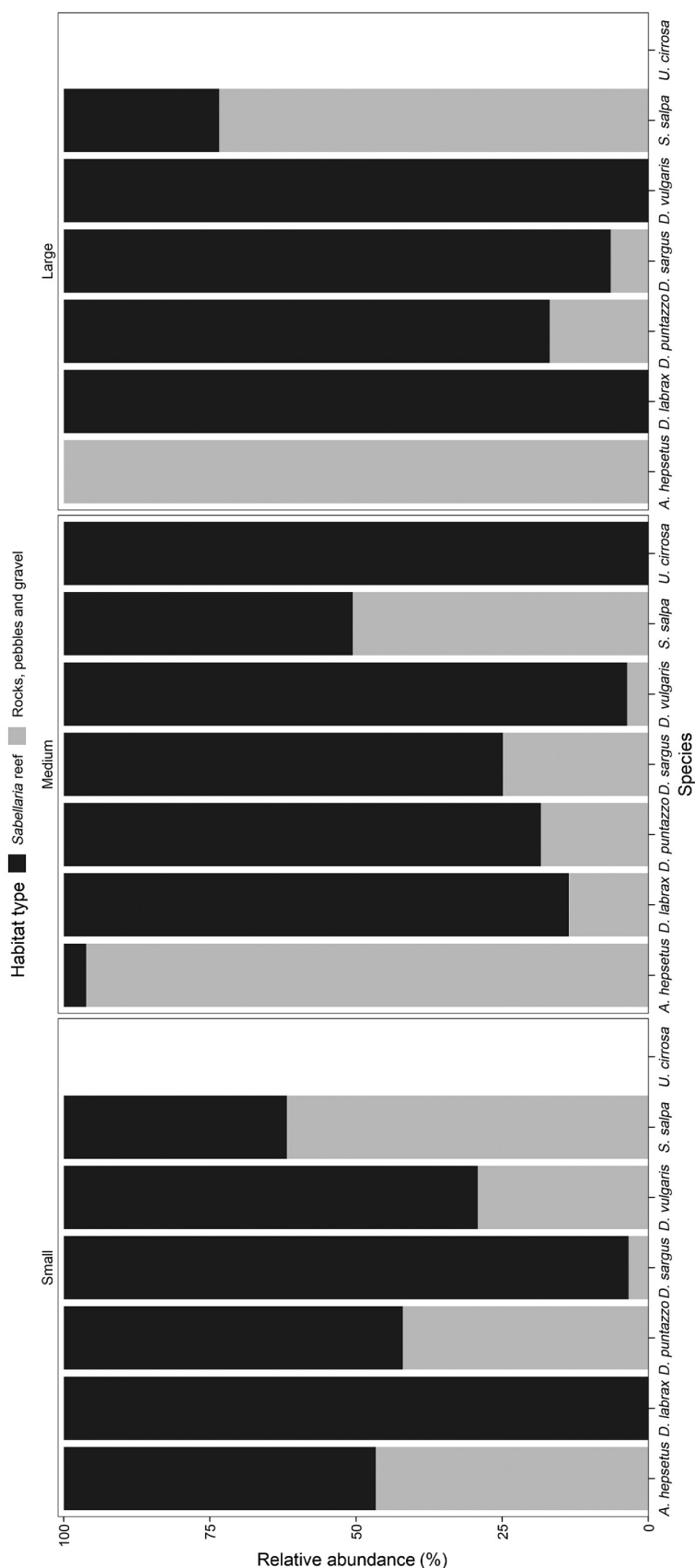
Fig. 8. Relative abundance (expressed as %) of the juveniles of 7 fish species recorded at the 3 study sites (S1−S3), according to habitat type (i.e. *Sabellaria alveolata* formations and other rocky substrates) and their size class (small, medium, large)

fishes with different behaviour (Kulbicki 1998, Pais & Cabral 2017), intra-observer variability due to divers' experience and habitat spatio-temporal variability and complexity (Friedlander & Parrish 1998, De Girolamo & Mazzoldi 2001, Green et al. 2013, Kislik et al. 2020). This latter aspect deserves particular attention in planning accurate UVC monitoring to estimate the specific associations between juvenile fish and microhabitats, likely occurring at small spatial scales (Harmelin-Vivien et al. 1995, Ventura et al. 2015, 2018b). In this context, recent mapping technologies based on ultra-high-resolution imagery acquired by small UAVs coupled with OBIA classification can be a valuable tool in identifying and characterizing coastal areas (Goncalves & Henriques 2015, Papakonstantinou et al. 2016, Ventura et al. 2016, 2018a, 2023, Jeong et al. 2018, Adade et al. 2021), providing accurate GIS data of heterogeneous stretches of coasts where the environmental variability of the seabed is a critical aspect capable of influencing the distribution of juvenile and adult fish assemblages. We demonstrated that the use of UAV-based cartography could be a valuable tool to integrate UVC surveys considering both the spatial planning of sampling campaigns and data acquisition of geomorphological features related to specific habitats such as sabellariid reefs that are characterized by high spatial 2D/3D heterogeneity, even at small spatial scales (Bertocci et al. 2017, Jackson-Bué et al. 2021, Ventura et al. 2021). The potential of UAVs for environmental assessment is increasingly being demonstrated, especially in monitoring programmes of shallow marine habitats, which are more and more frequently carried out using aerial UAV photography in conjunction with field surveys to map seagrass beds directly (Ventura et al. 2018a), submerged aquatic vegetation such as macroalgal beds (Rossiter et al. 2020, Ventura et al. 2023), coral reefs (Casella et al. 2017, Collin et al. 2018b, Nguyen et al. 2021), rocky reefs (Tait et al. 2021) and other biogenic reefs (Collin et al. 2019, Donnarumma et al. 2021, Bru-

nier et al. 2022). Mapping and monitoring these habitats may provide valuable information on fish—habitat associations, eventually helping to identify optimal monitoring designs and to establish the most effective schemes of temporal and spatial acquisition of data to achieve the specific objectives of the study, including, for example, the estimation of seasonal variability at target sites (Murphy & Jenkins 2010). Although topo-

graphic features (e.g. topographic position index, surface roughness, slope) derived from elevation data (digital elevation models) were not explicitly considered here, they could provide additional variables such as complementary fragmentation metrics or reef morphotype descriptors (Brunier et al. 2022) usable for the estimation of reef health status (Desroy et al. 2011, Bajjouk et al. 2020). However, our approach demonstrated that RGB orthophoto mosaic and polygon delineation in GIS could provide simple and relevant indicators of the shape and complexity of *Sabellaria* reefs related to their potential role as nursery grounds for juvenile fish.

5. CONCLUSIONS

Using UAV-based cartography reveals the potential for high-resolution remote sensing imagery to be incorporated into traditional UVC-based monitoring efforts by quantifying fine-scale attributes of biogenic reefs (Murfitt et al. 2017). The present study adds new perspectives to on-ground surveys, providing insight into the distribution and abundance of juvenile fishes associated with complex coastal habitats formed by reef-building polychaetes. The ability of UAVs to capture fine-scale (cm) georeferenced imagery of the whole reef, depicting morphological changes
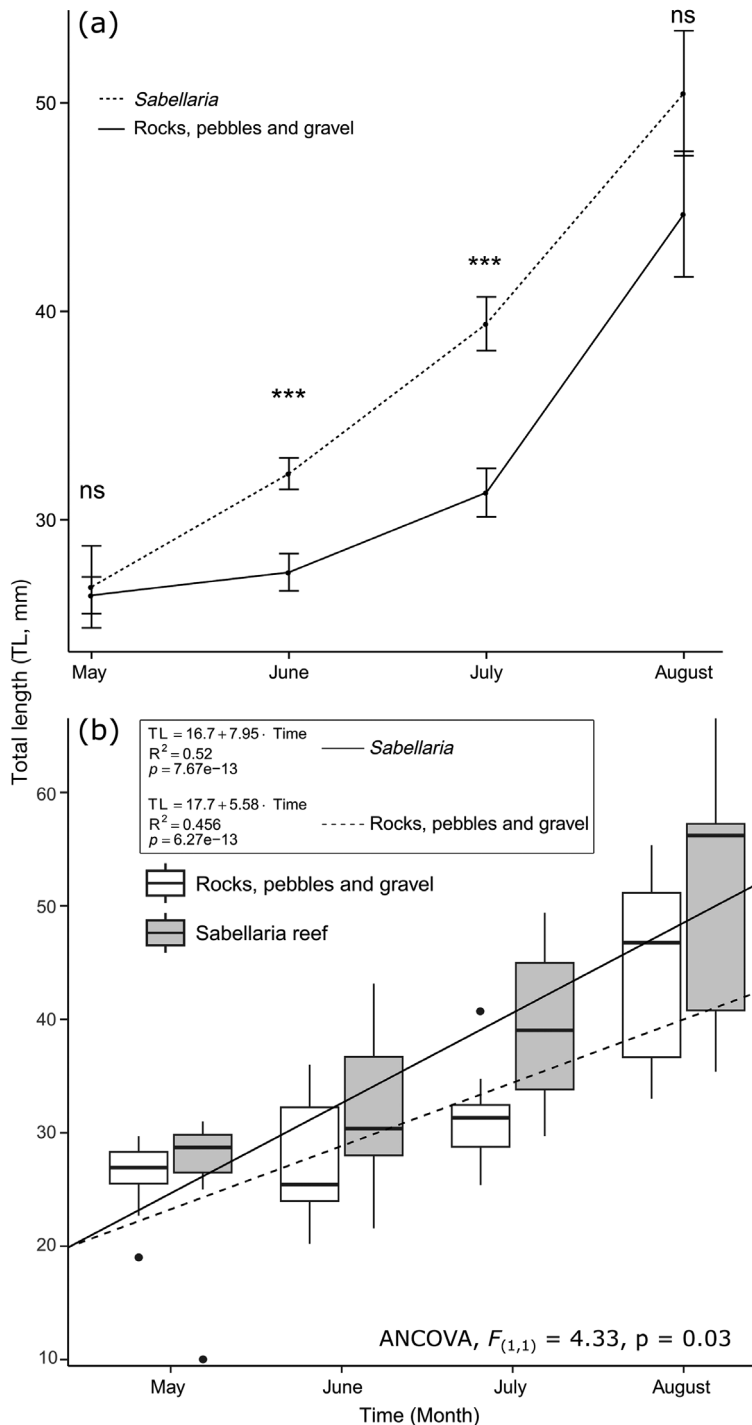

Fig. 9. Monthly mean size (total length, TL; mm ± SE) variation in *Diplodus sargus* juveniles (N = 173) according to preferential substrate type from the arrival of juveniles (May) until dispersal outside the surveyed sites (August). (a) Mean size variation over time (month). Wilcoxon signed-rank tests were used for pairwise comparisons. The alpha value was set at 0.05, and Bonferroni adjustment was applied for multiple comparisons (significance codes: ***p < 0.001; ns = non-significant). (b) TL with superimposed regression lines between the 2 substrate types reporting significant differences in slopes (rate of change in TL) tested with ANCOVA. Values per habitat type were obtained by combining all size measurements of sampled specimens from Sites S1 and S2 for *Sabellaria alveolata* reef and Site S3 for hard substrates (i.e. rocks, pebbles and gravel), respectively, over the entire 2 yr study period. Boundaries of the boxes represent the 25th and 75th percentiles; solid line within the box is the median; error bars above and below the box indicate the 90th and 10th percentiles, respectively; black points beyond the error bars represent the outliers
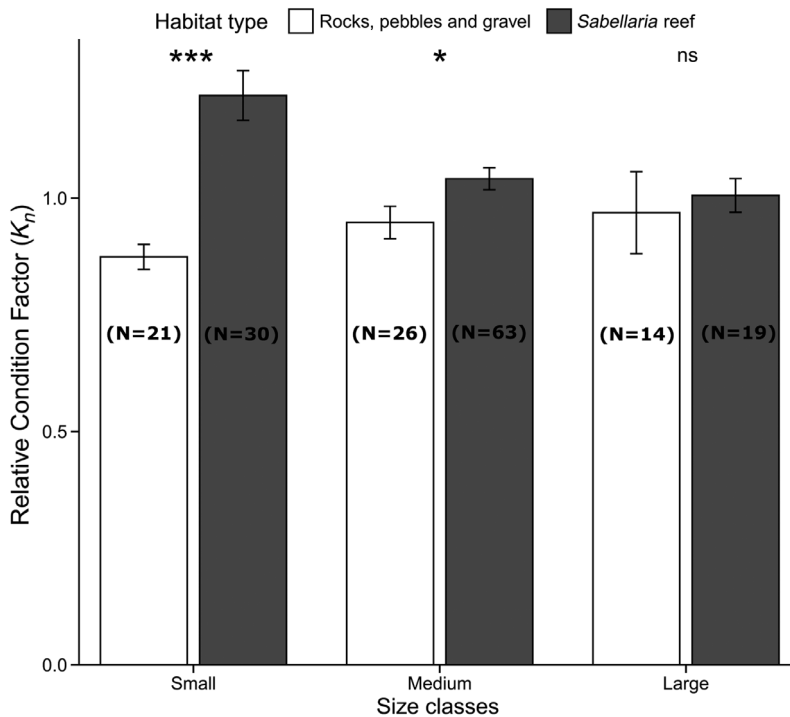
Fig. 10. Mean ± SE relative condition factor (K_n) of *Diplodus sargus* juveniles grouped by size class and habitat type. Wilcoxon signed-rank tests were used for pairwise comparisons. The alpha value was set at 0.05, and Bonferroni adjustment was applied for multiple comparisons. Significance codes: ***p < 0.001; *p < 0.05; ns = non-significant. Values in parentheses indicate sample sizes

findings can serve as a starting point for examining the effects of *S. alveolata* bioconstructions on juvenile fish assemblages, confirming that habitat structure should be included as a biodiversity component during evaluations of its nursery role, especially under the predicted increase in the impact of human activities and climate change on biogenic formations in the near future (Dubois et al. 2006, Curd et al. 2023).

occurring between accretion and erosion processes due to environmental dynamics, is crucial for improving spatial monitoring and assessing the spatial variability of reef habitat types. Although UAVs may not be able to fully replace *in situ* monitoring techniques on sabellariid reefs, they can provide complementary data suited to obtain a more comprehensive understanding of biogenic reef ecology and, in particular, their nursery role. Because the nursery role concept aims to identify high-quality areas, we encourage precise monitoring even of relatively small habitats, such as *Sabellaria* reefs presented here. Despite their limited size, they can represent essential nursery habitats that can support more adult recruits per unit of space compared to other habitats used by juveniles of the same species. This is a crucial aspect for prioritizing spatially explicit management (e.g. establishment of marine protected areas) when costs or other logistic constraints limit the amount of space that can be protected (Dahlgren et al. 2006). Finally, although this study is relatively limited in spatial coverage and temporal resolution and further studies are required to fully understand connectivity and ecological habitat linkages (Nagelkerken et al. 2015), our

LITERATURE CITED

Adade R, Aibinu AM, Ekumah B, Asaana J (2021) Unmanned aerial vehicle (UAV) applications in coastal zone management — a review. Environ Monit Assess 193:154

Ahlmann-Eltze C, Patil I (2021) ggsignif: R package for displaying significance brackets for 'ggplot2'. https://cloud.r-project.org/web/packages/ggsignif/index.html

Amara R, Meziane T, Gilliers C, Hermel G, Laffargue P (2007) Growth and condition indices in juvenile sole *Solea solea* measured to assess the quality of essential fish habitat. Mar Ecol Prog Ser 351:201—208

Anderson DR, Burnham KP, White GC (1998) Comparison of Akaike information criterion and consistent Akaike information criterion for model selection and statistical inference from capture-recapture studies. J Appl Stat 25:263—282

Aviz D, dos Santos CRM, Rosa Filho JS (2021) Sabellariid (Polychaeta: Annelida) reefs as nursery ground for the hermit crab *Clibanarius symmetricus* (Randall, 1840) on the Amazonian coast of Brazil. Mar Biol Res 17:21—30

Bajjouk T, Jauzein C, Drumetz L, Dalla Mura M, Duval A, Dubois SF (2020) Hyperspectral and lidar: complementary tools to identify benthic features and assess the ecological status of *Sabellaria alveolata* reefs. Front Mar Sci 7:575218

Baker R, Sheaves M (2007) Shallow-water refuge paradigm: conflicting evidence from tethering experiments in a tropical estuary. Mar Ecol Prog Ser 349:13—22

Beck MW, Heck KL, Able KW, Childers DL and others (2001) The identification, conservation, and management of estuarine and marine nurseries for fish and invertebrates: A better understanding of the habitats that serve as nurseries for marine species and the factors that create site-specific variability in nursery quality will improve conservation and management of these areas. BioScience 51:633—641

Beck MW, Heck KL Jr, Able KW, Childers DL and others (2003) The role of nearshore ecosystems as fish and shellfish nurseries. Issues Ecol 11

Bertocci I, Badalamenti F, Lo Brutto S, Mikac B and others (2017) Reducing the data-deficiency of threatened European habitats: spatial variation of sabellariid worm reefs and associated fauna in the Sicily Channel, Mediterranean Sea. Mar Environ Res 130:325—337

Biagi F, Sartor P, Ardizzone GD, Belcari P, Belluscio A, Serena F (2002) Analysis of demersal fish assemblages of the Tuscany and Latium coasts (north-western Mediterranean). Sci Mar 66:233—242

Bohnsack JA, Bannerot SP (1986) A stationary visual census technique for quantitatively assessing community structure of coral reef fishes. NOAA Tech Rep NMFS 41

Bonifazi A, Ventura D, Mancini E (2018) *Sabellaria* reefs as reservoirs of preferential species: the case of *Eulalia ornata* Saint-Joseph, 1888 (Annelida: Phyllodocidae). Mar Freshw Res 69:1635—1640

Bonifazi A, Lezzi M, Ventura D, Lisco S, Cardone F, Gravina MF (2019) Macrofaunal biodiversity associated with different developmental phases of a threatened Mediterranean *Sabellaria alveolata* (Linnaeus, 1767) reef. Mar Environ Res 145:97—111

Borghese J, Arduini D, Schimmenti E, Iaciofano D and others (2022) Assessment of the *Sabellaria alveolata* reefs' structural features along the Southern coast of Sicily (Strait of Sicily, Mediterranean Sea). Mediterr Mar Sci 23:890—899

Brandl SJ, Emslie MJ, Ceccarelli DMT, Richards Z (2016) Habitat degradation increases functional originality in highly diverse coral reef fish assemblages. Ecosphere 7: e01557

Bremec C, Carcedo C, Piccolo MC, Dos Santos E, Fiori S (2013) *Sabellaria nanella* (Sabellariidae): from solitary subtidal to intertidal reef-building worm at Monte Hermoso, Argentina (39°S, south-west Atlantic). J Mar Biol Assoc UK 93:81—86

Brock VE (1954) A preliminary report on a method of estimating reef fish populations. J Wildl Manag 18:297—308

Brunier G, Oiry S, Gruet Y, Dubois SF, Barillé L (2022) Topographic analysis of intertidal polychaete reefs (*Sabellaria alveolata*) at a very high spatial resolution. Remote Sens 14:307

Cantafaro A, Ardizzone G, Enea M, Ligas A, Colloca F (2017) Assessing the importance of nursery areas of European hake (*Merluccius merluccius*) using a body condition index. Ecol Indic 81:383—389

Casella E, Collin A, Harris D, Ferse S and others (2017) Mapping coral reefs using consumer-grade drones and structure from motion photogrammetry techniques. Coral Reefs 36:269—275

Chabot D, Dillon C, Ahmed O, Shemrock A (2017) Object-based analysis of UAS imagery to map emergent and submerged invasive aquatic vegetation: a case study. J Unmanned Veh Syst 5:27—33

Cheal AJ, Emslie MJ, Currey-Randall LM, Heupel MR (2021) Comparability and complementarity of reef fish measures from underwater visual census (UVC) and baited remote underwater video stations (BRUVS). J Environ Manag 289: 112375

Christensen MS (1978) Trophic relationships in juveniles of three species of sparid fishes in the South African marine littoral. Fish Bull 76:389—401

Cocheret De La Morinière E, Pollux BJA, Nagelkerken I, Van Der Velde G (2002) Post-settlement life cycle migration patterns and habitat preference of coral reef fish that use seagrass and mangrove habitats as nurseries. Estuar Coast Shelf Sci 55:309—321

Collin A, Etienne S, Feunteun E (2017) VHR coastal bathymetry using WorldView-3: colour versus learner. Remote Sens Lett 8:1072—1081

Collin A, Dubois S, Ramambason C, Etienne S (2018a) Very high-resolution mapping of emerging biogenic reefs using airborne optical imagery and neural network: the honeycomb worm (*Sabellaria alveolata*) case study. Int J Remote Sens 39:5660—5675

Collin A, Ramambason C, Pastol Y, Casella E and others (2018b) Very high resolution mapping of coral reef state using airborne bathymetric LiDAR surface-intensity and drone imagery. Int J Remote Sens 39:5676—5688

Collin A, Dubois S, James D, Houet T (2019) Improving intertidal reef mapping using UAV surface, red edge, and near-infrared data. Drones 3:67

Copp GH, Kovác V (1996) When do fish with indirect development become juveniles? Can J Fish Aquat Sci 53: 746—752

Costa C, Cataudella S (2007) Relationship between shape and trophic ecology of selected species of sparids of the Caprolace coastal lagoon (Central Tyrrhenian sea). Environ Biol Fishes 78:115—123

Costanza R, Arge R, De Groot R, Farberk S and others (1997) The value of the world's ecosystem services and natural capital. Nature 387:253—260

Curd A, Pernet F, Corporeau C, Delisle L, Firth LB, Nunes FLD, Dubois SF (2019) Connecting organic to mineral: how the physiological state of an ecosystem-engineer is linked to its habitat structure. Ecol Indic 98:49—60

Curd A, Chevalier M, Vasquez M, Boyé A and others (2023) Applying landscape metrics to species distribution model predictions to characterize internal range structure and associated changes. Glob Change Biol 29:631—647

Curtis LA (1975) Distribution of *Sabellaria vulgaris* Verrill (Polychaeta: Sabellariidae) on a sandflat in Delaware Bay. Chesap Sci 16:14—19

Dahlgren CP, Kellison GT, Adams AJ, Gillanders BM and others (2006) Marine nurseries and effective juvenile habitats: concepts and applications. Mar Ecol Prog Ser 312:291—295

Dance MA, Rooker JR (2016) Stage-specific variability in habitat associations of juvenile red drum across a latitudinal gradient. Mar Ecol Prog Ser 557:221—235

De Girolamo M, Mazzoldi C (2001) The application of visual census on Mediterranean rocky habitats. Mar Environ Res 51:1—16

Deias C, Guido A, Sanfilippo R, Apollaro C and others (2023) Elemental fractionation in Sabellariidae (Polychaeta) biocement and comparison with seawater pattern: a new environmental proxy in a high-biodiversity ecosystem? Water 15:1549

Desroy N, Dubois SF, Fournier J, Ricquiers L and others (2011) The conservation status of *Sabellaria alveolata* (L.) (Polychaeta: Sabellariidae) reefs in the Bay of Mont-Saint-Michel. Aquat Conserv Mar Freshw Ecosyst 21:462—471

Dias AS, Paula JJJ (2001) Associated fauna of *Sabellaria alveolata* colonies on the central coast of Portugal. J Mar Biol Assoc UK 81:169—170

Donnarumma L, D'Argenio A, Sandulli R, Russo GF, Chemello R (2021) Unmanned aerial vehicle technology to assess the state of threatened biogenic formations: the vermetid reefs of Mediterranean intertidal rocky coasts. Estuar Coast Shelf Sci 251:107228

Dorenbosch M, Van Riel MC, Nagelkerken I, Van der Velde G (2004) The relationship of reef fish densities to the proximity of mangrove and seagrass nurseries. Estuar Coast Shelf Sci 60:37—48

Dubois S, Retière C, Olivier F (2002) Biodiversity associated with *Sabellaria alveolata* (Polychaeta: Sabellariidae) reefs: effects of human disturbances. J Mar Biol Assoc UK 82: 817—826

Dubois S, Barillé L, Retière C (2003) Efficiency of particle retention and clearance rate in the polychaete *Sabellaria alveolata* L. C R Biol 326:413—421

Dubois S, Commito JA, Olivier F, Retière C (2006) Effects of epibionts on *Sabellaria alveolata* (L.) biogenic reefs and their associated fauna in the Bay of Mont Saint-Michel. Estuar Coast Shelf Sci 68:635—646

Edgar GJ, Barrett NS, Morton AJ (2004) Biases associated with the use of underwater visual census techniques to quantify the density and size-structure of fish populations. J Exp Mar Biol Ecol 308:269—290

Egerton JP, Johnson AF, Turner J, LeVay L, Mascareñas-Osorio I, Aburto-Oropeza O (2018) Hydroacoustics as a tool to examine the effects of Marine Protected Areas and habitat type on marine fish communities. Sci Rep 8:47

ESRI (2011) ArcGIS desktop: release 10. Environmental Systems Research Institute, Redlands, CA

Ferraton F, Harmelin-Vivien M, Mellon-Duval C, Souplet A (2007) Spatio-temporal variation in diet may affect condition and abundance of juvenile European hake in the Gulf of Lions (NW Mediterranean). Mar Ecol Prog Ser 337:197—208

Firth LB, Mieszkowska N, Grant LM, Bush LE and others (2015) Historical comparisons reveal multiple drivers of decadal change of an ecosystem engineer at the range edge. Ecol Evol 5:3210—3222

Firth LB, Curd A, Hawkins SJ, Knights AM and others (2021) On the diversity and distribution of a data deficient habitat in a poorly mapped region: the case of *Sabellaria alveolata* L. in Ireland. Mar Environ Res 169:105344

Foody GM (2020) Explaining the unsuitability of the kappa coefficient in the assessment and comparison of the accuracy of thematic maps obtained by image classification. Remote Sens Environ 239:111630

Francour P (1997) Fish assemblages of *Posidonia oceanica* beds at Port-Cros (France, NW Mediterranean): assessment of composition and long-term fluctuations by visual census. Mar Ecol 18:157—173

Franzitta G, Colletti A, Savinelli B, Lo Martire M, Corinaldesi C, Musco L (2022) Feasibility of the sabellarid reef habitat restoration. Front Mar Sci 9:854986

Friedlander AM, Parrish JD (1998) Habitat characteristics affecting fish assemblages on a Hawaiian coral reef. J Exp Mar Biol Ecol 224:1—30

García-Rubies A, Macpherson E (1995) Substrate use and temporal pattern of recruitment in juvenile fishes of the Mediterranean littoral. Mar Biol 124:35—42

Giangrande A, Gambi MC, Gravina MF (2020) Polychaetes as habitat former: structure and function. In: Rossi S, Bramanti L (eds) Perspectives on the marine animal forests of the world. Springer, Cham, p 219—237

Gibb N, Tillin HM, Pearce B, Tyler-Walters H (2014) Assessing the sensitivity of *Sabellaria spinulosa* to pressures associated with marine activities. JNCC Rep No. 504. Joint Nature Conservation Committee, Peterborough

Goncalves JA, Henriques R (2015) UAV photogrammetry for topographic monitoring of coastal areas. ISPRS J Photogramm Remote Sens 104:101—111

Gravina MF, Cardone F, Bonifazi A, Bertrandino MS and others (2018) *Sabellaria spinulosa* (Polychaeta, Annelida) reefs in the Mediterranean Sea: habitat mapping, dynamics and associated fauna for conservation management. Estuar Coast Shelf Sci 200:248—257

Gravina MF, Bonifazi A, Del Pasqua M, Giampaoletti J, Lezzi M, Ventura D, Giangrande A (2020) Perception of changes in marine benthic habitats: The relevance of taxonomic and ecological memory. Diversity 12:480—495

Green SJ, Tamburello N, Miller SE, Akins JL, Côté IM (2013) Habitat complexity and fish size affect the detection of Indo-Pacific lionfish on invaded coral reefs. Coral Reefs 32:413—421

Guisan A, Zimmermann NE (2000) Predictive habitat distribution models in ecology. Ecol Modell 135:147—186

Habitat Directive (1992) Council Directive 92/43/EEC of 21 May 1992 on the conservation of natural habitats and of wild fauna and flora. Official J EU 206(7):50

Harmelin-Vivien ML, Harmelin JG, Chauvet C, Duval C and others (1985) Evaluation visuelle des peuplements et populations de poissons: méthodes et problèmes. Rev Ecol (Terre Vie) 40:467—539

Harmelin-Vivien ML, Harmelin JG, Leboulleux V (1995) Microhabitat requirements for settlement of juvenile sparid fishes on Mediterranean rocky shores. Hydrobiologia 300—301:309—320

Heck KL Jr, Hays G, Orth RJ (2003) Critical evaluation of the nursery role hypothesis for seagrass meadows. Mar Ecol Prog Ser 253:123—136

Ingrosso G, Abbiati M, Badalamenti F, Bavestrello G and others (2018) Mediterranean bioconstructions along the Italian coast. Adv Mar Biol 79:61—136

Jackson EL, Rowden AA, Attrill MJ, Bossey SJ, Jones MB (2001) The importance of seagrass beds as a habitat for fishery species. Oceanogr Mar Biol Annu Rev 39:269—304

Jackson-Bué T, Williams GJ, Walker-Springett G, Rowlands SJ, Davies AJ (2021) Three-dimensional mapping reveals scale-dependent dynamics in biogenic reef habitat structure. Remote Sens Ecol Conserv 7:621—637

Jeong E, Park JY, Hwang CS (2018) Assessment of UAV photogrammetric mapping accuracy in the beach environment. J Coast Res 85:176—180

Jones AG, Dubois SF, Desroy N, Fournier J (2018) Interplay between abiotic factors and species assemblages mediated by the ecosystem engineer *Sabellaria alveolata* (Annelida: Polychaeta). Estuar Coast Shelf Sci 200:1—18

Jones AG, Denis L, Fournier J, Desroy N, Duong G, Dubois SF (2020) Linking multiple facets of biodiversity and ecosystem functions in a coastal reef habitat. Mar Environ Res 162:105092

Jones AG, Dubois SF, Desroy N, Fournier J (2021) Intertidal ecosystem engineer species promote benthic—pelagic coupling and diversify trophic pathways. Mar Ecol Prog Ser 660:119—139

Jones T, Davidson RJ, Gardner JPA, Bell JJ (2015) Evaluation and optimisation of underwater visual census monitoring

for quantifying change in rocky-reef fish abundance. Biol Conserv 186:326—336

Kassambara A (2020) ggpubr: 'ggplot2' based publication ready plots. R package version 0.4.0. https://cran.r-project.org/web/packages/ggpubr/index.html

Kenny AJ, Cato I, Desprez M, Fader G, Schüttenhelm RTE, Side J (2003) An overview of seabed-mapping technologies in the context of marine habitat classification. ICES J Mar Sci 60:411—418

Kislik C, Genzoli L, Lyons A, Kelly M (2020) Application of UAV imagery to detect and quantify submerged filamentous algae and rooted macrophytes in a non-wadeable river. Remote Sens 12:3332

Kulbicki M (1998) How the acquired behaviour of commercial reef fishes may influence the results obtained from visual censuses. J Exp Mar Biol Ecol 222:11—30

La Manna G, Guala I, Grech D, Perretti F and others (2021) Performance of a baited underwater video system vs. the underwater visual census technique in assessing the structure of fish assemblages in a Mediterranean marine protected area. Mediterr Mar Sci 22:480—495

Le Cam JBB, Fournier J, Etienne S, Couden J (2011) The strength of biogenic sand reefs: visco-elastic behaviour of cement secreted by the tube building polychaete *Sabellaria alveolata*, Linnaeus, 1767. Estuar Coast Shelf Sci 91:333—339

Le Pape O, Bonhommeau S (2015) The food limitation hypothesis for juvenile marine fish. Fish Fish 16:373—398

Lefcheck JS, Hughes BB, Johnson AJ, Pfirrmann BW and others (2019) Are coastal habitats important nurseries? A meta-analysis. Conserv Lett 12:e12645

Lindsay JB (2014) The whitebox geospatial analysis tools project and open-access GIS. In: Proceedings of the GIS Research UK 22nd Annual Conference, Glasgow, 16—18 April 2014. The University of Glasgow, p 1—8

Lisco S, Moretti M, Moretti V, Cardone F, Corriero G, Longo C (2017) Sedimentological features of *Sabellaria spinulosa* biocontructions. Mar Pet Geol 87:203—212

Litvin SY, Weinstein MP, Sheaves M, Nagelkerken I (2018) What makes nearshore habitats nurseries for nekton? An emerging view of the nursery role hypothesis. Estuar Coasts 41:1539—1550

Lloret J, Gil de Sola L, Souplet A, Galzin R (2002) Effects of large-scale habitat variability on condition of demersal exploited fish in the north-western Mediterranean. ICES J Mar Sci 59:1215—1227

Macpherson E (1998) Ontogenetic shifts in habitat use and aggregation in juvenile sparid fishes. J Exp Mar Biol Ecol 220:127—150

Méndez Casariego A, Schwindt E, Iribarne O (2004) Evidence of habitat structure-generated bottleneck in the recruitment process of the SW Atlantic crab *Cyrtograpsus angulatus*. Mar Biol 145:259—264

Moretti M, Lisco S, Brandano M, Tomassetti L, Gravina MF, Pantaloni M, Console F (2019) The *Sabellaria* bioconstructions and their Plio-Pleistocene substratum along the southern Latium coast (Tor Caldara, Anzio, Italy). In: Viglio M, Tropeano M, Pascucci V, Ruber D, Sabato L (eds) 34th IAS Meeting of Sedimentology, Rome, 10—13 September 2019. International Association of Sedimentologists, Ghent, p 10—13

Muller A, Poitrimol C, Nunes FLD, Boyé A and others (2021) Musical chairs on temperate reefs: Species turnover and replacement within functional groups explain regional diversity variation in assemblages associated with honeycomb worms. Front Mar Sci 8:654141

Muller A, Dubois SF, Boyé A, Becheler R and others (2023) Environmental filtering and biotic interactions act on different facets of the diversity of benthic assemblages associated with eelgrass. Ecol Evol 13:e10159

Mumby PJ, Edwards AJ, Ernesto Arias-Gonzalez J, Lindeman KC and others (2004) Mangroves enhance the biomass of coral reef fish communities in the Caribbean. Nature 427:533—536

Murfitt SL, Allan BM, Bellgrove A, Rattray A, Young MA, Ierodiaconou D (2017) Applications of unmanned aerial vehicles in intertidal reef monitoring. Sci Rep 7:10259

Murphy HM, Jenkins GP (2010) Observational methods used in marine spatial monitoring of fishes and associated habitats: a review. Mar Freshw Res 61:236—252

Nagelkerken I (2009) Evaluation of nursery function of mangroves and seagrass beds for tropical decapods and reef fishes: patterns and underlying mechanisms. In: Nagelkerken I (ed) Ecological connectivity among tropical coastal ecosystems. Springer, Dordrecht, p 357—399

Nagelkerken I, Roberts CM, van der Velde G, Dorenbosch M, van Riel MC, Cocheret de la Moriniere E, Nienhuis PH (2002) How important are mangroves and seagrass beds for coral-reef fish? The nursery hypothesis tested on an island scale. Mar Ecol Prog Ser 244:299—305

Nagelkerken I, Sheaves M, Baker R, Connolly RM (2015) The seascape nursery: a novel spatial approach to identify and manage nurseries for coastal marine fauna. Fish Fish 16:362—371

Nguyen T, Liquet B, Mengersen K, Sous D (2021) Mapping of coral reefs with multispectral satellites: a review of recent papers. Remote Sens 13:4470

Olán-González M, Briones-Fourzán P, Lozano-Álvarez E, Acosta-González G, Alvarez-Filip L (2023) Similar functional composition of fish assemblages despite contrasting levels of habitat degradation on shallow Caribbean coral reefs. PLOS ONE 18:e0295238

Pais MP, Cabral HN (2017) Fish behaviour effects on the accuracy and precision of underwater visual census surveys. A virtual ecologist approach using an individual-based model. Ecol Modell 346:58—69

Pais MP, Cabral HN (2018) Effect of underwater visual survey methodology on bias and precision of fish counts: a simulation approach. PeerJ 6:e5378

Papakonstantinou A, Topouzelis K, Pavlogeorgatos G (2016) Coastline zones identification and 3D coastal mapping using UAV spatial data. ISPRS Int J Geo-Inf 5:75

Paterson AW, Whitfield AK (2000) Do shallow-water habitats function as refugia for juvenile fishes? Estuar Coast Shelf Sci 51:359—364

Pearce B, Hill JM, Grubb L, Harper G (2011a) Impacts of marine aggregate extraction on adjacent *Sabellaria spinulosa* aggregations and other benthic fauna. MEPF 08/P39. Marine Ecological Survey, Bath

Pearce B, Hill JM, Wilson C, Griffin R, Earnshaw S, Pitts J (2011b) *Sabellaria spinulosa* reef ecology and ecosystem services. Reef Ecosystems Ecology Report. Crown Estate, London

Rabaut M, Vincx M, Degraer S (2009) Do *Lanice conchilega* (sandmason) aggregations classify as reefs? Quantifying habitat modifying effects. Helgol Mar Res 63:37—46

Rabaut M, Van de Moortel L, Vincx M, Degraer S (2010) Biogenic reefs as structuring factor in *Pleuronectes platessa* (plaice) nursery. J Sea Res 64:102—106

Reise K (2012) Tidal flat ecology: an experimental approach to species interactions. Ecological Studies, Vol 54. Springer-Verlag, Berlin

Ribeiro C, Almeida AJ, Araújo R, Biscoito M, Freitas M (2005) Fish assemblages of Cais do Carvao Bay (Madeira Island) determined by the visual census technique. J Fish Biol 67:1568—1584

Rossiter T, Furey T, McCarthy T, Stengel DB (2020) UAV-mounted hyperspectral mapping of intertidal macroalgae. Estuar Coast Shelf Sci 242:106789

Ruiz GM, Hines AH, Posey MH (1993) Shallow water as a refuge habitat for fish and crustaceans in non-vegetated estuaries: an example from Chesapeake Bay. Mar Ecol Prog Ser 99:1—16

Russo T, Costa C, Cataudella S (2007) Correspondence between shape and feeding habit changes throughout ontogeny of gilthead sea bream *Sparus aurata* L., 1758. J Fish Biol 71:629—656

Sala E, Ballesteros E (1997) Partitioning of space and food resources by three fish of the genus *Diplodus* (Sparidae) in a Mediterranean rocky infralittoral ecosystem. Mar Ecol Prog Ser 152:273—283

Sale PF, Douglas WA (1981) Precision and accuracy of visual census technique for fish assemblages on coral patch reefs. Environ Biol Fishes 6:333—339

Sanfilippo R, Serio D, Deias C, Rosso A (2022) *Sabellaria alveolata* (Annelida, Polychaeta) bioconstructions and associated macroalgal community from Portopalo di Capo Passero (SE Sicily). Mediterr Mar Sci 23:150—156

Schloesser RW, Fabrizio MC (2019) Nursery habitat quality assessed by the condition of juvenile fishes: not all estuarine areas are equal. Estuar Coasts 42:548—566

Searcy SP, Eggleston DB, Hare JA (2007) Is growth a reliable indicator of habitat quality and essential fish habitat for a juvenile estuarine fish? Can J Fish Aquat Sci 64:681—691

Seitz RD, Wennhage H, Bergström U, Lipcius RN, Ysebaert T (2014) Ecological value of coastal habitats for commercially and ecologically important species. ICES J Mar Sci 71:648—665

Sheaves M, Baker R, Johnston R (2006) Marine nurseries and effective juvenile habitats: an alternative view. Mar Ecol Prog Ser 318:303—306

St. John J, Russ GR, Gladstone W (1990) Accuracy and bias of visual estimates of numbers, size structure and biomass of a coral reef fish. Mar Ecol Prog Ser 64:253—262

Stone R, Callaway R, Bull JC (2019) Are biodiversity offsetting targets of ecological equivalence feasible for biogenic reef habitats? Ocean Coast Manag 177:97—111

Tait LW, Orchard S, Schiel DR (2021) Missing the forest and the trees: utility, limits and caveats for drone imaging of coastal marine ecosystems. Remote Sens 13:3136

Tillin HM, Marshall C, Gibb N (2018) *Sabellaria spinulosa*, didemnids and other small ascidians on tide-swept moderately wave-exposed circalittoral rock. In: Tyler-Walters H, Hiscock K (eds) Marine Life Information Network: biology and sensitivity key information reviews [online]. Marine Biological Association of the United Kingdom, Plymouth

Tiralongo F, Mancini E, Ventura D, de Malerbe S and others (2021) Commercial catches and discards composition in the central Tyrrhenian Sea: a multispecies quantitative and qualitative analysis from shallow and deep bottom trawling. Mediterr Mar Sci 22:521—531

Ventura D, Jona Jona Lasinio G, Ardizzone G (2015) Temporal partitioning of microhabitat use among four juvenile fish species of the genus *Diplodus* (Pisces: Perciformes, Sparidae). Mar Ecol 36:1013—1032

Ventura D, Bruno M, Jona Lasinio G, Belluscio A, Ardizzone G (2016) A low-cost drone based application for identifying and mapping of coastal fish nursery grounds. Estuar Coast Shelf Sci 171:85—98

Ventura D, Bonhomme V, Colangelo P, Bonifazi A, Jona Lasinio G, Ardizzone G (2017) Does morphology predict trophic niche differentiation? Relationship between feeding habits and body shape in four co-occurring juvenile species (Pisces: Perciformes, Sparidae). Estuar Coast Shelf Sci 191:84—95

Ventura D, Bonifazi A, Gravina MF, Belluscio A, Ardizzone G (2018a) Mapping and classification of ecologically sensitive marine habitats using unmanned aerial vehicle (UAV) imagery and object-based image analysis (OBIA). Remote Sens 10:1331

Ventura D, Bonifazi A, Jona Lasinio G, Gravina MF, Mancini E, Ardizzone G (2018b) Can microscale habitat-related differences influence the abundance of ectoparasites? Multiple evidences from two juvenile coastal fish (Perciformes: Sparidae). Estuar Coast Shelf Sci 209: 110—122

Ventura D, Dubois SF, Bonifazi A, Jona Lasinio G, Seminara M, Gravina MF, Ardizzone G (2021) Integration of close-range underwater photogrammetry with inspection and mesh processing software: a novel approach for quantifying ecological dynamics of temperate biogenic reefs. Remote Sens Ecol Conserv 7:169—186

Ventura D, Napoleone F, Cannucci S, Alleaume S, Valentini E, Casoli E, Burrascano S (2022) Integrating low-altitude drone based-imagery and OBIA for mapping and manage [sic] semi natural grassland habitats. J Environ Manag 321:115723

Ventura D, Grosso L, Pensa D, Casoli E and others (2023) Coastal benthic habitat mapping and monitoring by integrating aerial and water surface low-cost drones. Front Mar Sci 9:1096594

Vigliola L, Harmelin-Vivien M (2001) Post-settlement ontogeny in three Mediterranean reef fish species of the genus *Diplodus*. Bull Mar Sci 68:271—286

Vigliola L, Harmelin-Vivien ML, Biagi F, Galzin R and others (1998) Spatial and temporal patterns of settlement among sparid fishes of the genus *Diplodus* in the northwestern Mediterranean. Mar Ecol Prog Ser 168:45—56

Wentworth CK (1922) A scale of grade and class terms for clastic sediments. J Geol 30(5):377—392

Wetz JJ, Ajemian MJ, Shipley B, Stunz GW (2020) An assessment of two visual survey methods for documenting fish community structure on artificial platform reefs in the Gulf of Mexico. Fish Res 225:105492

Wood SN (2001) mgcv: GAMs and generalized ridge regression for R. R News 1:20—25

Wood S (2015) Package 'mgcv'. R package version 1.7-29. https://cran.r-project.org/web/packages/mgcv/index. html

Zuur AF, Ieno EN, Smith GM (2007) Analysing ecological data. Springer, New York, NY